Fast Electron Transport

Core Heating Simulation for Fast Ignition

T. Johzaki

A. Sunahara[A], H. Nagatomo, C.-B. Cai[*], H. Sakagami[B], K. Mima[**],

and FIREX Project group

ILE Osaka University,

[A]Institute for Laser Technology,

[B]National Institute for Fusion Science

*** Present address, IAPCM China**

**** Also, Graduate School for the Creation of New Photonics Industries and Universidad Politecnica de Madrid**

ILE, Osaka Univ.

2nd UK-Japan Winter School in High Energy Density Science, Royal Observatory, Edinburgh, UK, 5-7, January 2011.

Contents

Evaluation of Core Heating Properties with 2D PIC + FP simulations

1. **Modeling**
2. **B-field effects on core heating & Dependence of Cone Tip on Heating Performance(IFSA2008, PoP 16, 062706 (2009))**
3. **Pre-plasma effects on core heating in cone-guiding fast ignition (FIW2010, APS2010, IAEA Proc. http://www-pub.iaea.org/MTCD/Meetings/PDFplus/2010/cn180/cn180_papers/ife_p6-01.pdf)**
4. **New concept "extended double cone" for improving core heating performance (FIW2010, APS2010, IAEA Proc. http://www-pub.iaea.org/MTCD/Meetings/PDFplus/2010/cn180/cn180_papers/ife_p6-01.pdf)**
5. **Resistive Guiding ---Tongari Cone**

1. Simulation modeling for Fokker-Planck code “FIBMET”

Fast electron transport; 2-D FP code “FIBMET”

“FIBMET”

Bulk Plasma: 1-fluid 2-temperature hydro model

- EOS
  - ✓Electron … Thomas Fermi
  - ✓Ion ……. Cowan’s model
- Energy Transport
  - ✓Electron conduction; Spitzer-Harm’s Flux-limited diffusion
  - ✓Radiation Transport; multi-group flux-limited diffusion
  - ✓3.52MeV α-particles; multi-group flux-limited diffusion
  - ✓**Fast electron; Relativistic Fokker-Planck model**

Self-generated electric and magnetic fields

Generalized Ohm’s Law for bulk electrons, the Ampere-Maxwell eq. and Faraday’s Law

$$\vec{E} = \vec{u_b} \times \vec{B} + \frac{\eta}{\mu_0}\nabla \times \vec{B} - \eta \vec{j_f} - \frac{1}{en_e}\vec{j_f} \times \vec{B} - \frac{1}{en_e}\nabla p_e$$

$$\frac{\partial \vec{B}}{\partial t} = \nabla \times \left(\vec{u}_e \times \vec{B}\right) - \nabla \times \left(\frac{\eta}{\mu_0}\nabla \times \vec{B}\right) + \nabla \times \left(\eta \vec{j}_f\right) + \nabla \times \left(\frac{1}{en_e}\vec{j}_f \times \vec{B}\right) + \nabla \times \left(\frac{1}{en_e}\nabla p_{be}\right)$$

① $\eta\left(\nabla \times \vec{j}_f\right)$

② $\nabla\eta \times \vec{j}_f$

η : resistivity

$\vec{j}_f$: fast electron current density

ILE Osaka

Relativistic Fokker-Planck Equation

$$\frac{\partial f}{\partial t} + \frac{\vec{p}}{\gamma m_e}\cdot\nabla f + q\left(\vec{E} + \frac{\vec{p}}{\gamma m_e}\times\vec{B}\right)\cdot\frac{\partial f}{\partial \vec{p}} = \sum_j C_{collison}\left(f, f_j\right) + S \quad (j = e, i)$$

1. **Collision terms**

   free electrons, bounded electrons, ions
2. **Numerical scheme**
3. **Field Model**

Collision terms in Relativistic Fokker-Planck Eq. (1)

Coulomb interaction between fast electron and bulk “free” electron

Short range ---------- $b \leqslant \lambda_D$

Long range ---------- $b > \lambda_D \ \left(k < k_D\right)$
(Corrective response)

≒ Excitation of quasi static wave (Langmuir wave)

Treatment of interaction

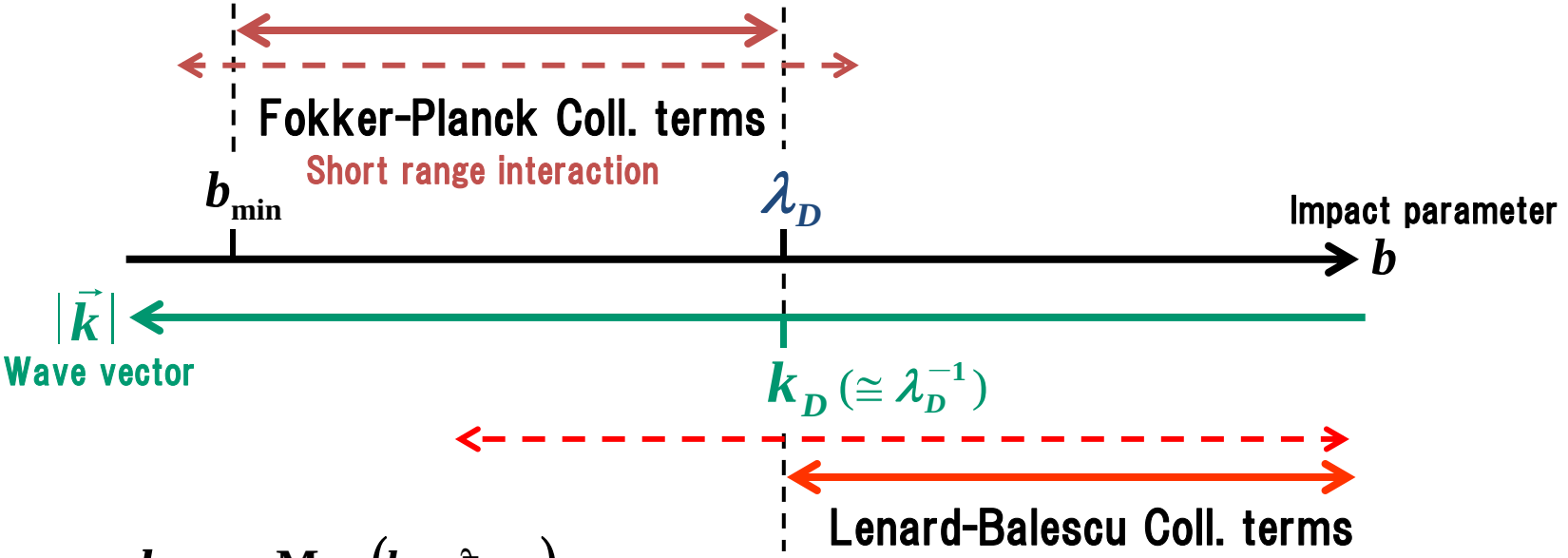

$b_{\min} = \mathrm{Max}\left(b_L, \lambda\!\!\!^{-}_{DB}\right)$

Long range corrective effects are described via dielectric function.

Collision terms in Relativistic Fokker-Planck Eq. (2)

◎ FP Collision terms; relativistic modification for Coulomb Logarithm

Instead of Rutherford cross section, Møllerer cross section is used.

Application range

$$\lambda\!\!\!^{-}_{DB} \leqslant b \leqslant \lambda_D$$

⇨

Logarithmic factor

$$\ln\Lambda_{Short} = \frac{1}{2}\left\{\ln\frac{1}{2\varepsilon^2} + \frac{1}{8}\left(\frac{\tau}{\tau+1}\right) - \frac{2\tau+1}{(\tau+1)^2}\ln 2 + 1 - \ln 2\right\}$$

where

$$\tau = \gamma - 1\,,\ \varepsilon = b_{\min}/b_{\max} \approx \left(\lambda\!\!\!^{-}_{DB}/2\right)/\lambda_D$$

◎ Inclusion of long range interaction

For LB collision terms, dielectric function is assumed as

$$\Longrightarrow\ \varepsilon = 1 - \omega_p^2/\omega^2$$

Integrated over $k < k_D\left(\cong \lambda_D^{-1}\right)$

⇨

Logarithmic factor

$$\ln\Lambda_{Long} = \frac{1}{2}\ln\left(\frac{2}{3}\frac{v^2}{\lambda_D^2\omega_p^2}\right) - \frac{1}{2}$$

$$\ln\Lambda_{RFP} \Rightarrow \ln\Lambda_{Short} + \ln\Lambda_{Long}$$

Collision terms in Relativistic Fokker-Planck Eq. (3)

◎ Interaction with "bounded" electrons

Imploded plasma・・・～fully ionized
Solid target・Au cone
・・・Partially ionized ⇒
Contribution of bound electrons is important.

Logarithmic factor (ICRU rep. v.37)

$$\ln\Lambda_{bound} = \frac{1}{2}\left\{\ln\frac{\tau^2(\gamma+1)}{2I^2} + 1 - \beta^2 - \frac{2\gamma-1}{\gamma^2}\ln 2 + \frac{1}{8}\left(\frac{\gamma-1}{\gamma}\right)^2\right\}$$

where $\tau = \gamma - 1, \quad \beta = v/c$

I : effective ionization potential(1)

$$I(Z^*) = I_0 \frac{\exp(1.29x^{0.72-0.18x})}{\sqrt{1-x}}$$

where $x = Z^*/Z, \quad I_0(Z) \approx a_0 Z^{(2)}, \quad a_0 = 10\text{eV}$

- Z : atomic number
- Z^* : ion charge (0 ~Z)
- I_0 : effective ionization potential for "cold" atom

※ Fermi degenerate effect is approximately included by $I = I + \mu_F$.

$$\sum_j C_{Bound}(f, f_j) = \frac{Y_B n_B}{m_e}\frac{m_e^2}{p^2}\frac{\partial}{\partial p}\left(\gamma^2 f\right) + \frac{1}{2}Y_B n_B \frac{m_e}{p^3}\left[\frac{\partial}{\partial\mu}\left\{\gamma\left(1-\mu^2\right)\frac{\partial f}{\partial\mu}\right\} + \frac{\gamma}{1-\mu^2}\frac{\partial^2 f}{\partial\omega^2}\right]$$

where $Y_B = 4\pi\left(e^2/4\pi\varepsilon_0\right)^2 \ln\Lambda_{Bound}$

$n_B = (Z - Z^*)n_i$

(1) Derived by R. More (1985) from the Thomas-Fermi model
(2) H. D. Betz (1980) ; H. H. Andersen and J. F. Ziegler (1977).

Comparison of Stopping Power for Fast Electrons

1MeV electron in solid density material

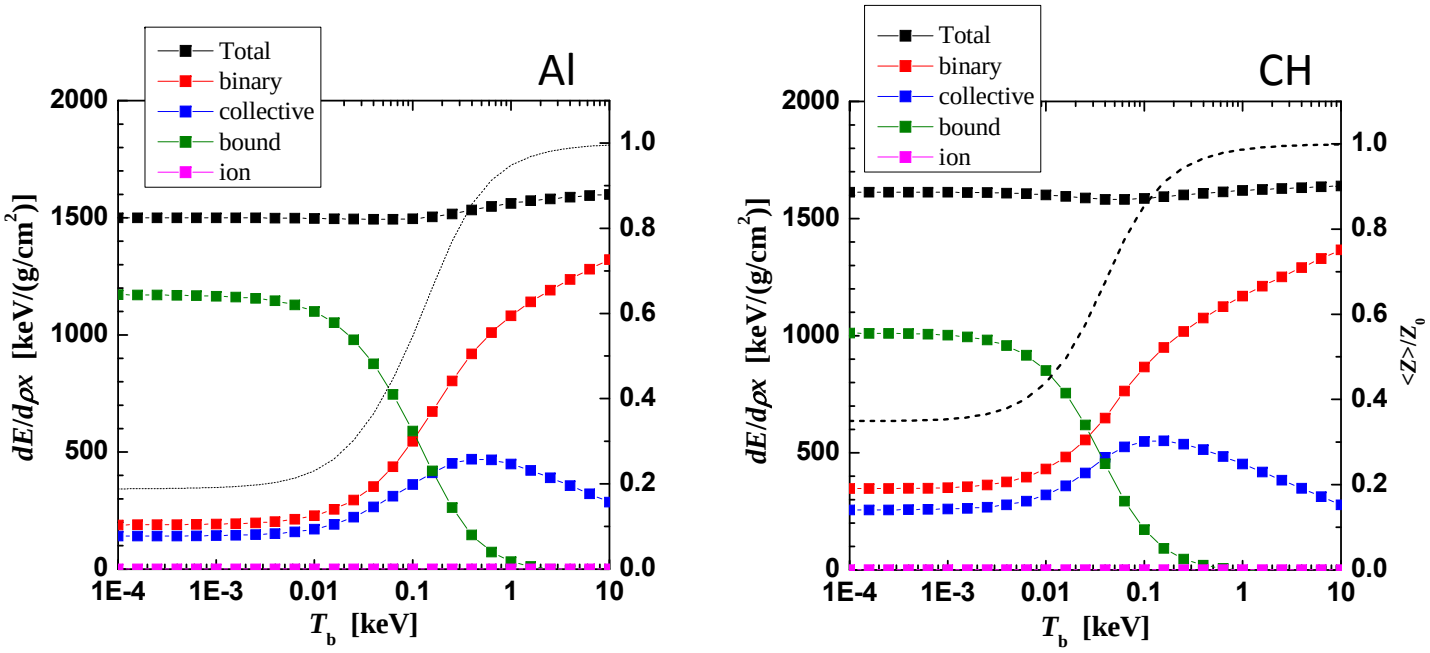

$$\left(\frac{dE}{dx}\right)_{e-e} = 4\pi e^4 \frac{Z^* n_i}{m_e} \frac{\gamma^2 m_e^2}{p^2} \left[\ln\Lambda_{bin} + \ln\Lambda_{coll} + \ln\Lambda_{bound}\right]$$

$$\begin{cases} \ln\Lambda_{bin} = \frac{1}{2}\left\{\ln\frac{1}{2\varepsilon^2} + \frac{1}{8}\left(\frac{\tau}{\tau+1}\right) - \frac{2\tau+1}{(\tau+1)^2}\ln 2 + 1 - \ln 2\right\} \\ \ln\Lambda_{coll} = \frac{1}{2}\ln\left(\frac{2}{3}\frac{v^2}{\lambda_D^2\omega_p^2}\right) - \frac{1}{2} \\ \ln\Lambda_{bound} = \frac{1}{2}\left\{\ln\frac{\tau^2(\gamma+1)}{2I^2} + 1 - \beta^2 - \frac{2\gamma-1}{\gamma^2}\ln 2 + \frac{1}{8}\left(\frac{\gamma-1}{\gamma}\right)^2\right\} \end{cases}$$

$$\begin{cases} \tau = \gamma - 1 \\ \varepsilon = b_{\min}/b_{\max} \approx (\lambda\!\!\!^{-}_{DB}/2)/\lambda_D \\ \beta = v/c \end{cases}$$

Collision terms in Relativistic Fokker-Planck Eq. (4)

◎ Interaction with bulk ions・・・Scattering

- **Impact parameter:** $b_0 = \hbar / p_e = \hbar m_e v_e$
- **Ion radius :** $a \sim 1.4 a_0 Z^{-1/3}, \quad a_0 = \hbar / m_e e^2 = 5.29 \times 10^{-9}$ [cm]
- **Debye length:** $\lambda_D = \sqrt{\dfrac{1}{4\pi e^2 n_e / T_e}}$

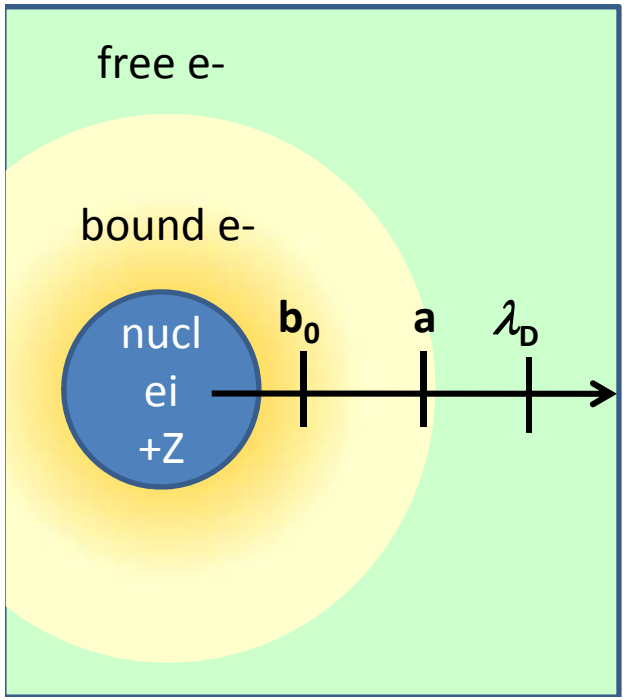

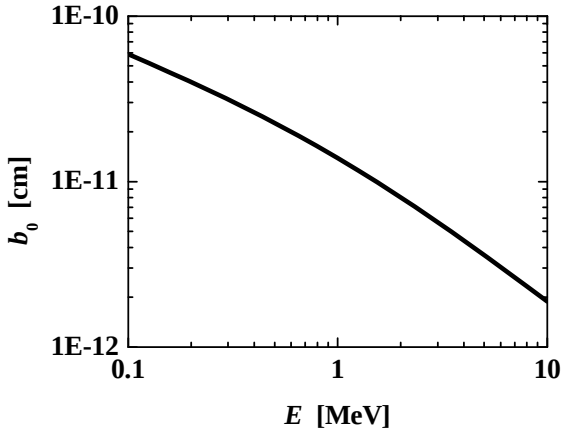

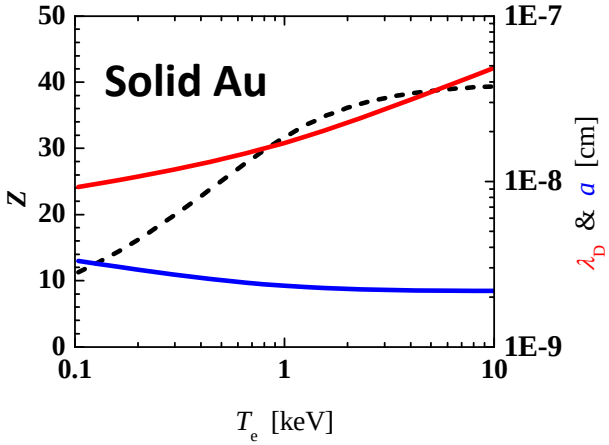

$b_0 < a < \lambda_D$

$b_0 < a$ interaction with un-shielded potential of nucleous inside of ion sphere

$a < \lambda_D$ Interaction with shielded potential of ion by bound electron

Collision terms in Relativistic Fokker-Planck Eq. (5)

◎ Interaction with partially-ionized ions…scattering

$$\nu_{ei} = \frac{4\pi e^4 n_i}{p^2 v}\left\{Z_i^2 \ln(\lambda_D/b_0)\right\}$$

without bounded e- (current model)

$$\nu_{ei} = \frac{4\pi e^4 n_i}{p^2 v}\left\{< \bar{Z}^2 > \ln(a/b_0) + Z_i^2 \ln(\lambda_D/a)\right\}$$

inside bounded e- *outside bounded e-*

radius of bounded e- cloud

$$a = 1.4 a_0 / Z_0^{1/3}$$

averaged unshielded charge

$$< \bar{Z}^2 >= \sum_{j=i+1}^{N} \frac{Z_j^2}{N-i}$$

Scattering rate normalized by fully ionized rate

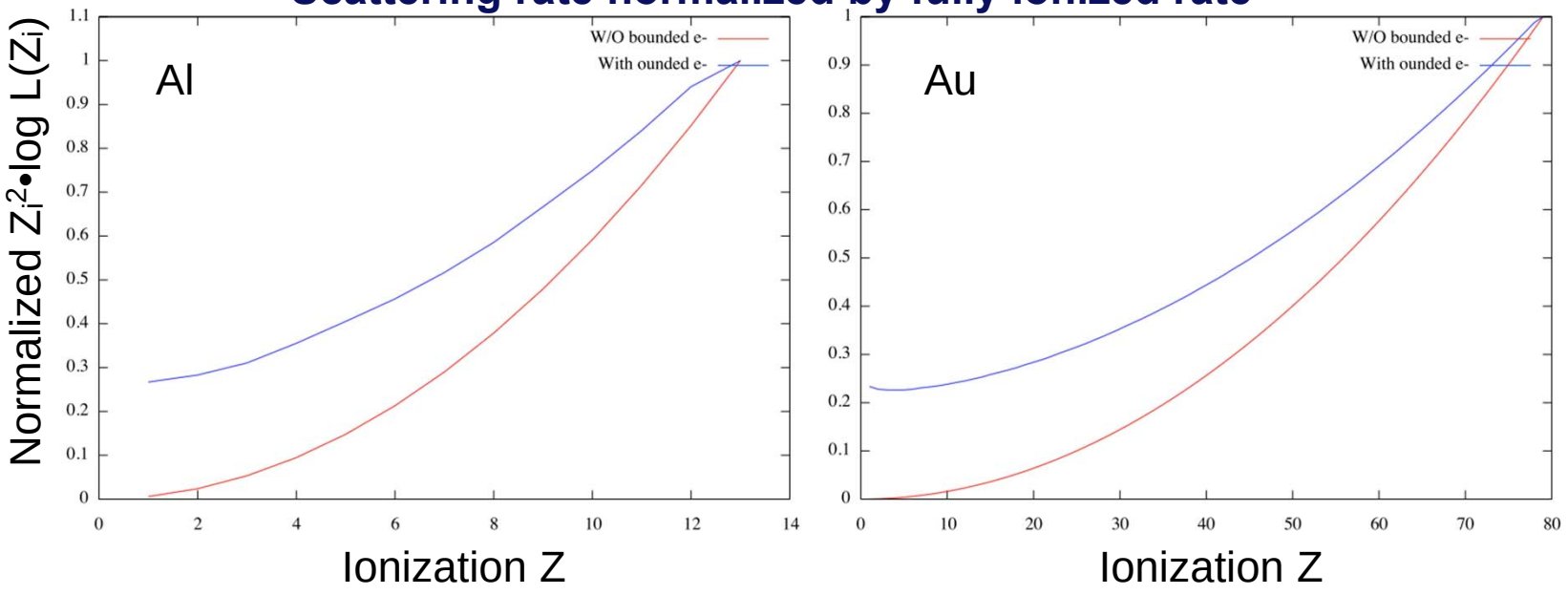

Even neutral atom scatters electrons with 20 ~ 30 % of fully ionized scattering rate.

Calculational Model for Electric & Magnetic fields

- **Ohm's law for bulk electrons ;** $\vec{E} - \vec{u}_b \times \vec{B} = \eta \vec{j}_b + \frac{1}{en_e} \vec{j}_b \times \vec{B} - \frac{1}{en_e} \nabla p_e$

  - **Total current ;** $\vec{j} = \vec{j}_f + \vec{j}_b$
  - **Ampere-Maxwell equation;** $\nabla \times \vec{B} = \mu_0 \vec{j} + \frac{1}{c^2} \frac{\partial \vec{E}}{\partial t} \approx \mu_0 \left(\vec{j}_f + \vec{j}_b \right)$

$$\Rightarrow \quad \vec{j}_b = \frac{1}{\mu_0} \nabla \times \vec{B} - \vec{j}_f$$

Electric field $\vec{E} = \vec{u}_b \times \vec{B} + \frac{\eta}{\mu_0} \nabla \times \vec{B} - \eta \vec{j}_f - \frac{1}{en_e} \vec{j}_f \times \vec{B} - \frac{1}{en_e} \nabla p_e$

- **Faraday's law;** $\nabla \times \vec{E} = -\frac{\partial \vec{B}}{\partial t}$

Magnetic field

$$\frac{\partial \vec{B}}{\partial t} = \nabla \times \left(\vec{u}_e \times \vec{B} \right) - \nabla \times \left(\frac{\eta}{\mu_0} \nabla \times \vec{B} \right) + \nabla \times \left(\eta \vec{j}_f \right) + \nabla \times \left(\frac{1}{en_e} \vec{j}_f \times \vec{B} \right) + \nabla \times \left(\frac{1}{en_e} \nabla p_{be} \right)$$

Resistive field

① $\eta \left(\nabla \times \vec{j}_f \right)$

② $\nabla \eta \times \vec{j}_f$

Thermo-electric field

Coupled Fokker-Planck Rad.-Hydro simulation model

2D Fokker-Planck + Hydro; "FIBMET"

Fast Electron Transport

Relativistic Fokker-Planck transport

$f(r,z,p,\mu,\omega)$: Fast electron distribution function

(r,z) – CIP

(p) – Discontinuous Linear FEM

(μ, ϕ) – 2D Discrete Ordinate Sn method

j_f

B_ϕ , E_x, E_y

Electromagnetic Fields

- Ohm's law for bulk electrons

$$\vec{E} - \vec{u}_b \times \vec{B} = \eta \vec{j}_b + \frac{1}{en_e}\vec{j}_b \times \vec{B} - \frac{1}{en_e}\nabla p_e$$

- Faraday's law

$$\nabla \times \vec{E} = -\frac{\partial \vec{B}}{\partial t}$$

B_ϕ , E_x, E_y (r, z)

ρ, T

Energy deposition rate

B_ϕ , E_x, E_y

T_e, n_e, u, v, η

Radiation-Hydrodynamics with fusion

Bulk Plasma; ρ, T_i, T_e, u, v(r,z)

- 1-fluid 2-temp. CIP code with thermal conduction + QEOS(Thomas-Fermi + Cowan's EOS)

Radiation; $\varepsilon_r(r,z,h\nu)$

- Multi group flux-limited diffusion

α-particle transport; $\phi_\alpha(r,z,E_\alpha)$

- Multi group flux-limited diffusion

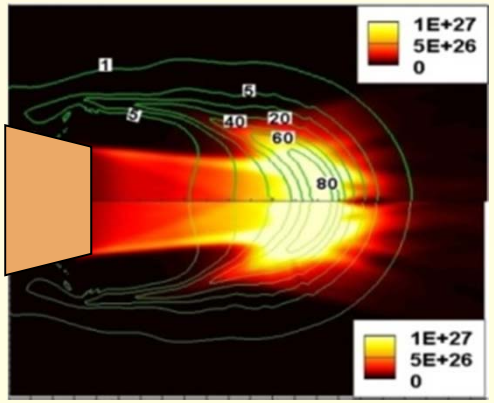

FI³ Project

Fast Ignition Integrated Interconnecting code Project

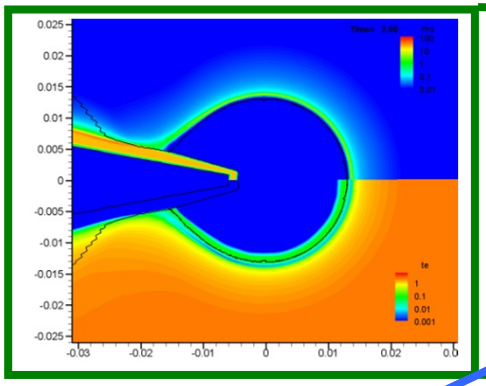

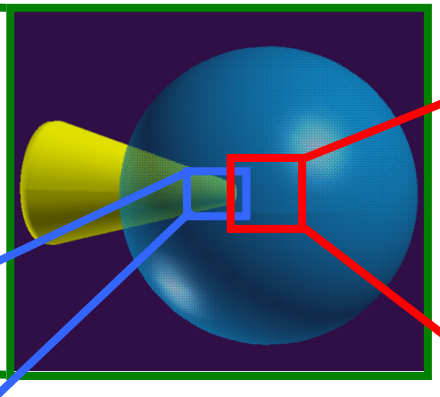

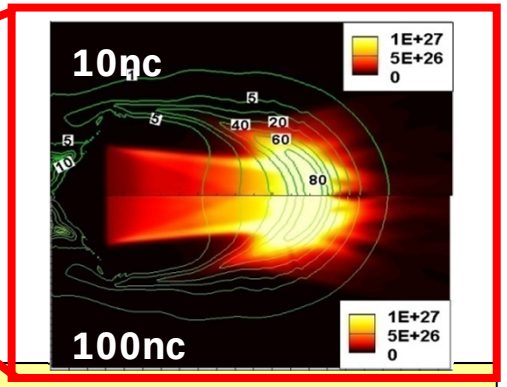

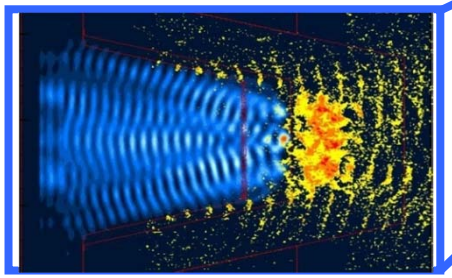

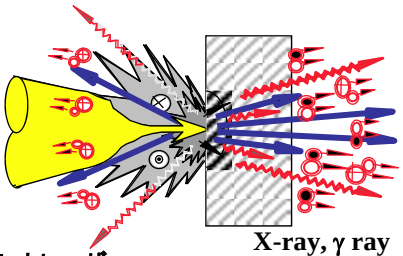

ペタワットレーザー

X-ray, γ ray
MeV 電子,
MeV イオン
中性子,中間子
陽電子

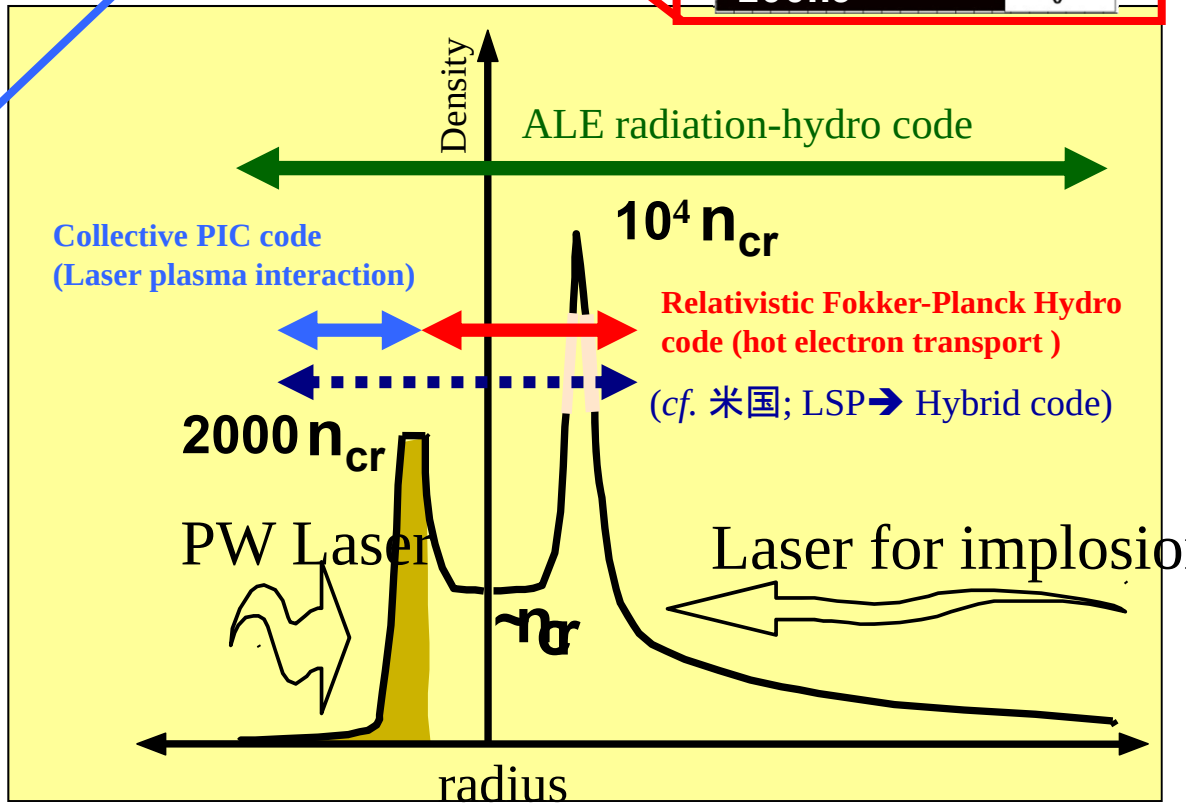

Integrated Simulations

$\mathcal{FI}^3$ (Fast Ignition Integrated Interconnecting) Code System

$\mathcal{FI}^3$

Radiation-Hydro "PINOCO"
(implosion)

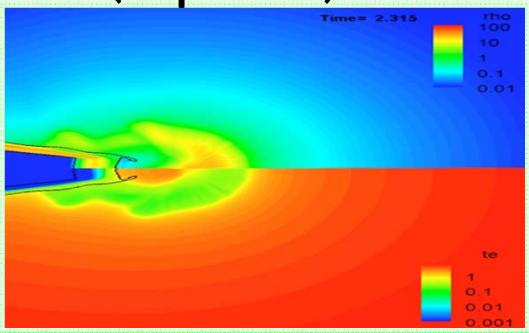

Radiation-Hydro "Star"
with 3D ray-trace & detailed atomic data
(pre-foamed plasma)

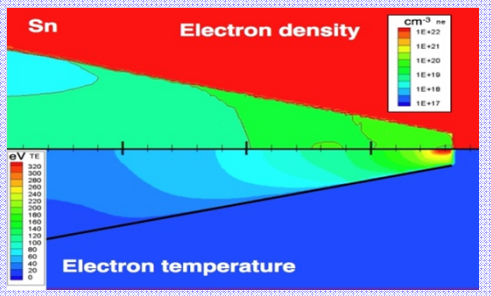

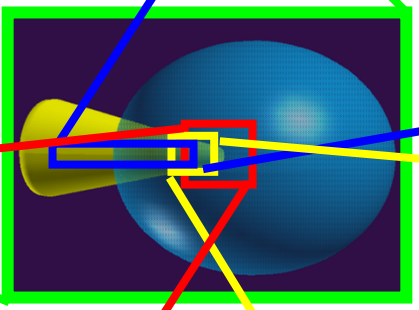

Imploded core & deformed cone profiles

Pre-formed plasma profile

FP-Hydro "FIBMET"
(core heating & fusion burning)

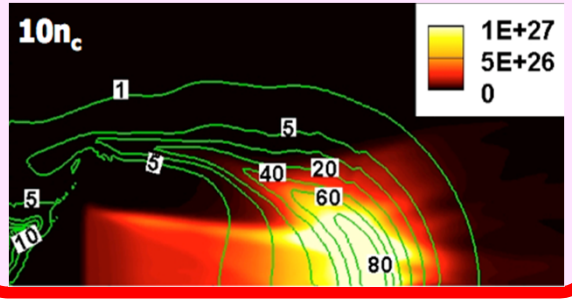

Fast electron & ion profiles

PIC "FISCOF"
(relativistic laser-plasma interaction)

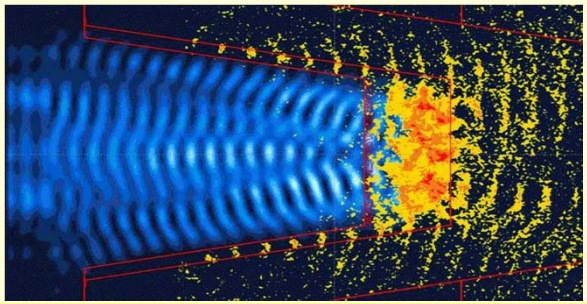

2. B-field effects on core heating & Dependence of heating performance on cone material

IFSA2008, PoP 16, 062706 (2009)

Core Heating Simulation w/o Cone Tip
Simulation condition

Core profile: CD core

ρ_0 = 200g/cm^3, Gaussian with r_{HWHM} = 10μm,

ρR_0 = 0.2g/cm^2, m_{fuel} = 2μg

Ti = Te = 0.4keV uniform

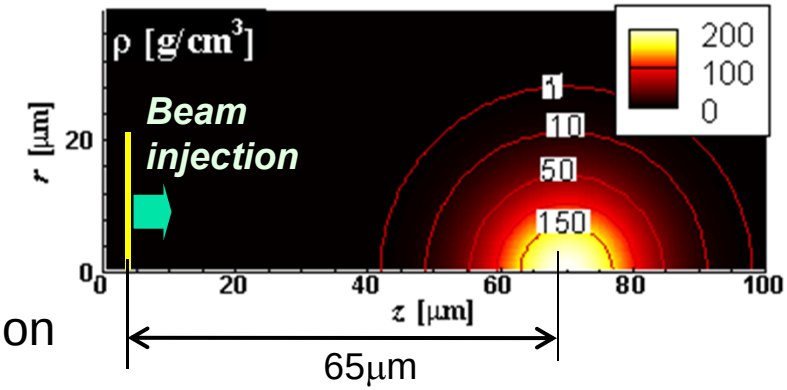

Fast electron beam

Injection; 65μm away from the core center.

Super Gaussian with r_{HWHM} = 15μm in r-direction

T_{fe} = 1.0MeV (slop temperature)

E_{fe} = 5kJ

τ_{fe} = 5ps

$P_h = E_{fe} / \tau_{fe}$ = 1 PW

I_h = 1.4 x10^{20}W/cm^2 at the central axis

B-fields effects on core heating

Results 1 / 2

IFSA2008, PoP 16, 062706 (2009)

The Fast electron beam: T_{fe} = 1.0 ,E_{fe} = 5kJ, τ_{fe} = 5ps

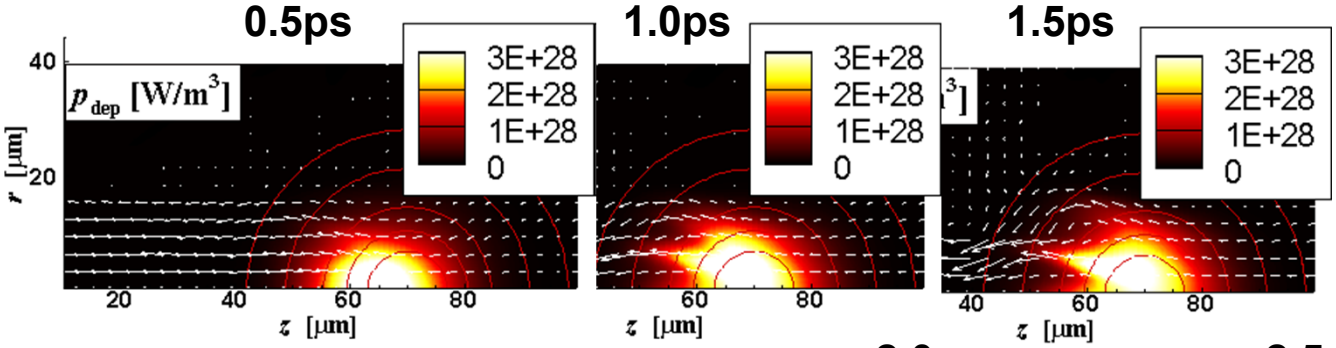

Initially, the core heating rate increases due to the beam pinching effect.

But, in the later phase, B-field due to $\nabla T_{ex} \nabla n_e$ grows, which scatters the fast electrons. Thus the heating rate starts to decrease.

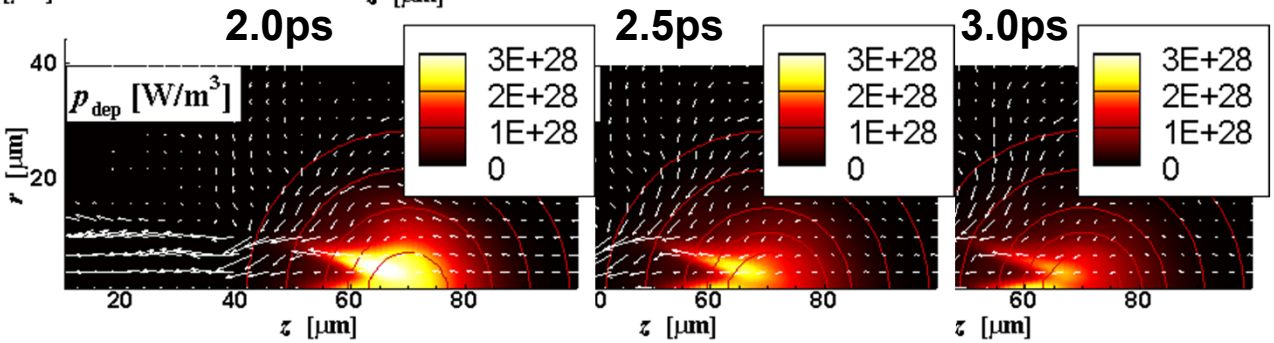

1ps

Beam pinching by B-field due to $\nabla \times (\eta j_f)$

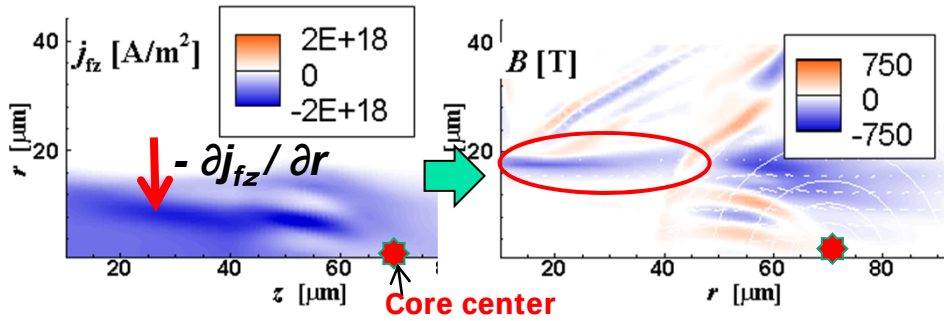

2ps

Beam scattering by B-field due to $\nabla T_e \times \nabla n_e$

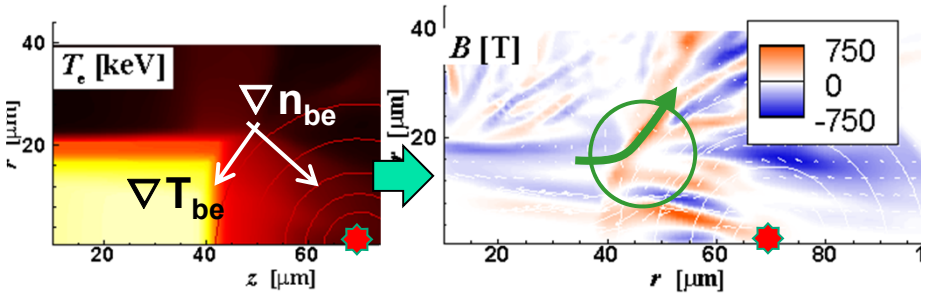

B-fields effects on core heating

Results 2 / 2

IFSA2008, PoP 16, 062706 (2009)

The Fast electron beam: T_{fe} = 1.0 ,E_{fe} = 5kJ, τ_{fe} = 5ps

Temporal evolution of (a) core heating rates and (b) $<T_i>_{DD}$

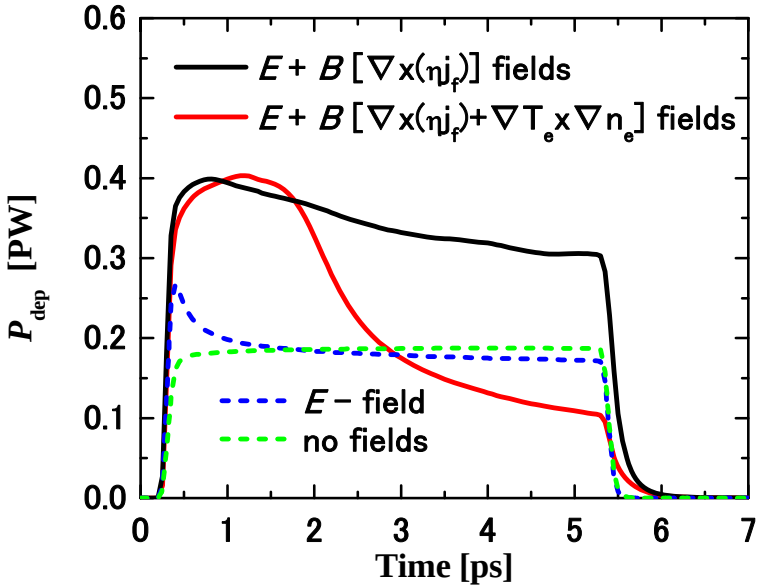

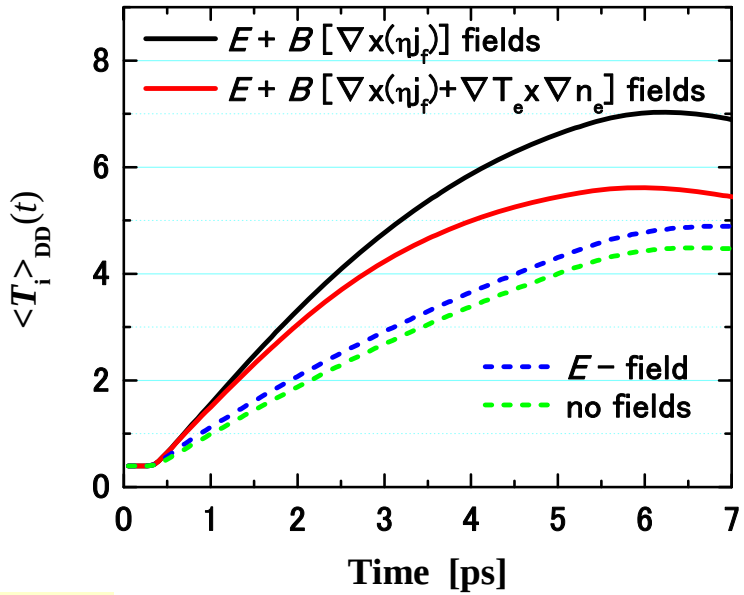

- If only $\nabla x(\eta j_f)$ is considered as the b-field source, Energy coupling from FE to Core $\eta_{fe\rightarrow core}$ is ~1.8 times higher than the case w/o fields.
- When B-field caused by ∇Te x ∇ne is included, $\eta_{fe\rightarrow core}$ becomes smaller by 20% compared with the case neglecting this field.
- (Even in this case, $\eta_{fe\rightarrow core}$ is 1.4 times larger than the case w/o fields).

Source E_{fe}	5kJ	
E_{dep} (E_{dep} /E_{fe})	1.50kJ	(30%)
due to Collision (/E_{dep})	1.38kJ	(92%)
due to Field (/E_{dep})	0.12kJ	(8%)
$<T_e>_{DD}$	5.87keV	
$<T_i>_{DD}$	4.94keV	
T_i local max	7.24keV	
Yn_{DD}	7.95e10	

IFSA2008, PoP 16, 062706 (2009)

Effects of Cone Tip

Fast electron transport : 2D Relativistic Fokker-Planck

- Short range binary collision & long range collective interactions are included.
- E-filed is evaluated by generalized Ohm's Law.
- Temporal evolution of B-field is calculated using Faraday's Law.

Bulk plasma: 1-fluid 2-temp. Hydro code + radiation, alpha-particle transport (multi-group diffusion)

Core Profiles

material **CD core with Au cone tip**

CD core:

$\rho_0 = 200 g/cm^3$, Gaussian with $r_{HWHM} = 10\mu m$,

Ti = Te = 0.4keV uniform

$m_{fuel} = 0.002mg$

Au cone :

$\rho_{cone} = 19.32 g/cm^3$, $T_{cone} = 0.05keV$

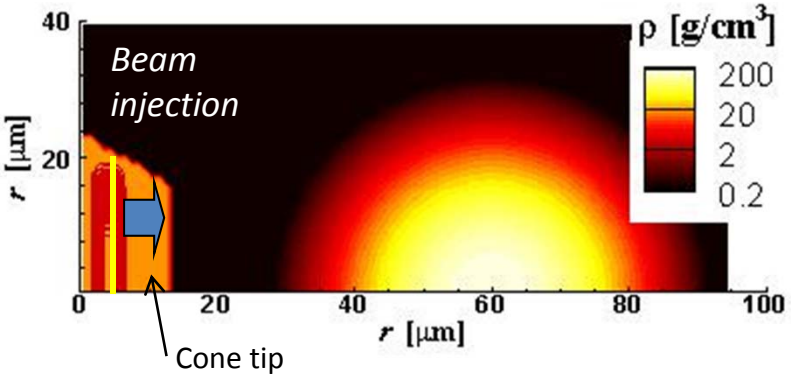

Fast electron beam

Injection point is 50μm away from the core center.

Super Gaussian with $r_{HWHM} = 15\mu m$ in r-direction

E_{fe} = 5kJ (50% coupling from LFEX laser to fast electron)

T_{fe} 1.0MeV (slop temperature)

τ_{fe} = 5 ps

$P_h = E_{fe} / \tau_{fe}$ = 1.0 (5ps) PW

$I_h = 1.4 \times 10^{20} W/cm^2$ at the central axis

IFSA2008, PoP 16, 062706 (2009)

Effects of Cone Tip
Results 1/2 Au –cone

Beam Intensity vs z (r < 20um) at 2ps

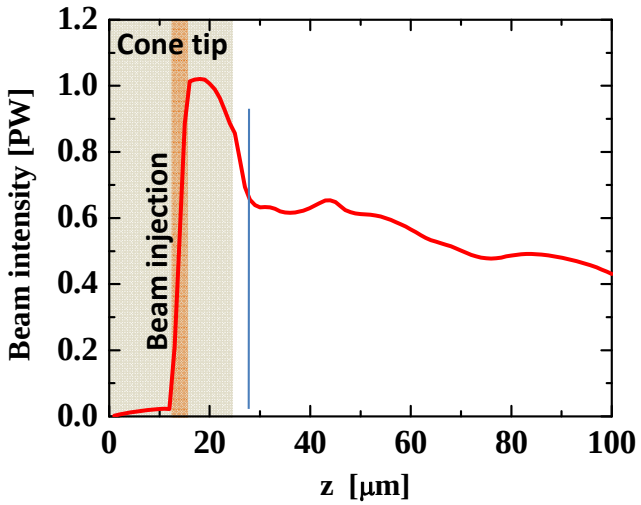

Angular spread source, out of tip (x < 20um) at 2ps

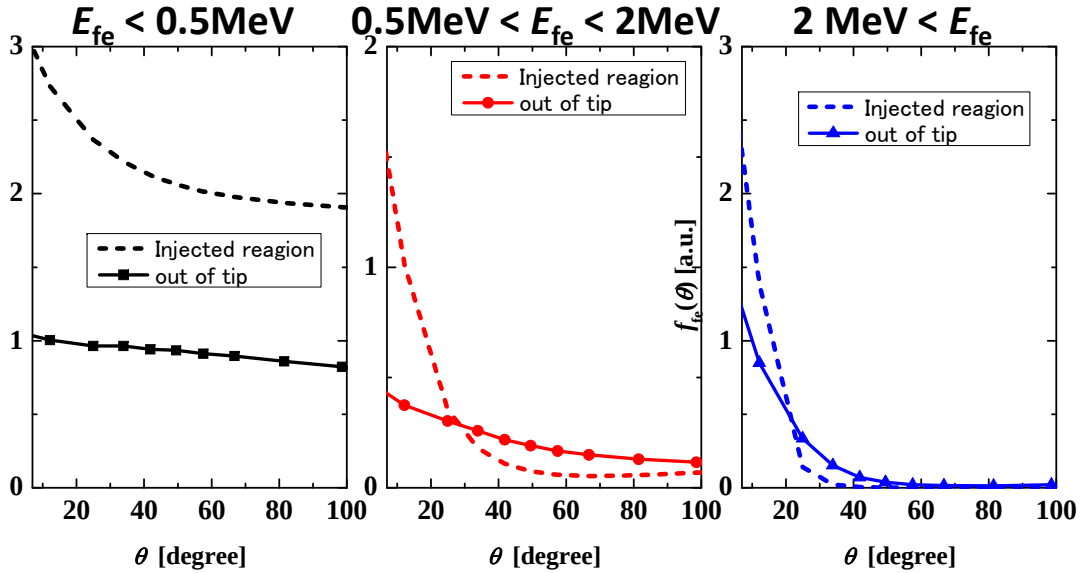

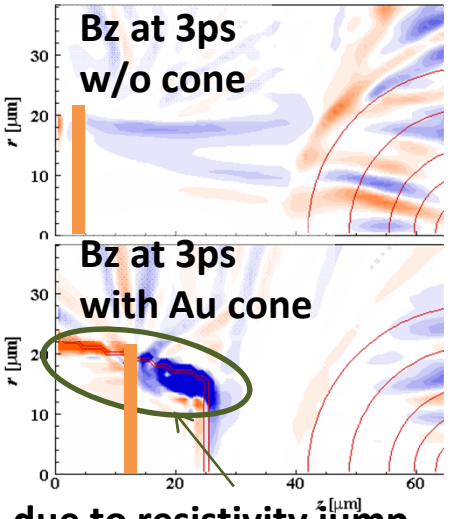

due to resistivity jump

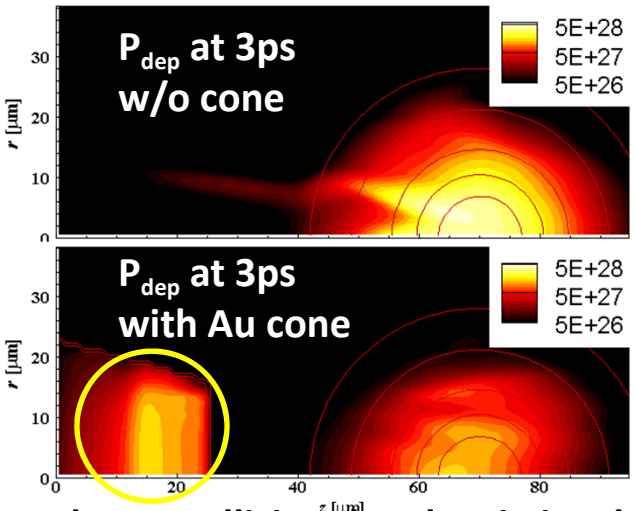

due to collisional and resistive drag

Case	E_{dep} core ($\eta_{fe\rightarrow core}$)	$\langle T_e \rangle_{max}$	$\langle T_i \rangle_{max}$
w/o cone	1.50 kJ (30.0%)	7.12 keV	5.62 keV
Au cone	**0.77 kJ (15.4%) (49%↓)**	**3.87 keV**	**3.38 keV (40%↓)**

IFSA2008, PoP 16, 062706 (2009)

Effects of Cone Tip

Results 2/2 cone-tip material dependence

Material	ρ_{solid} [g/cm^3]	<Z>	n_e /cm^3 (fully ionized case)
CH	1.0	3.5	1.68e23
Al	2.70	13	7.78e23
Cu	8.96	29	2.45e24
Au	19.32	79	4.64e24

Small

Collisional effects
(stopping, scattering, resistive fields)

Large

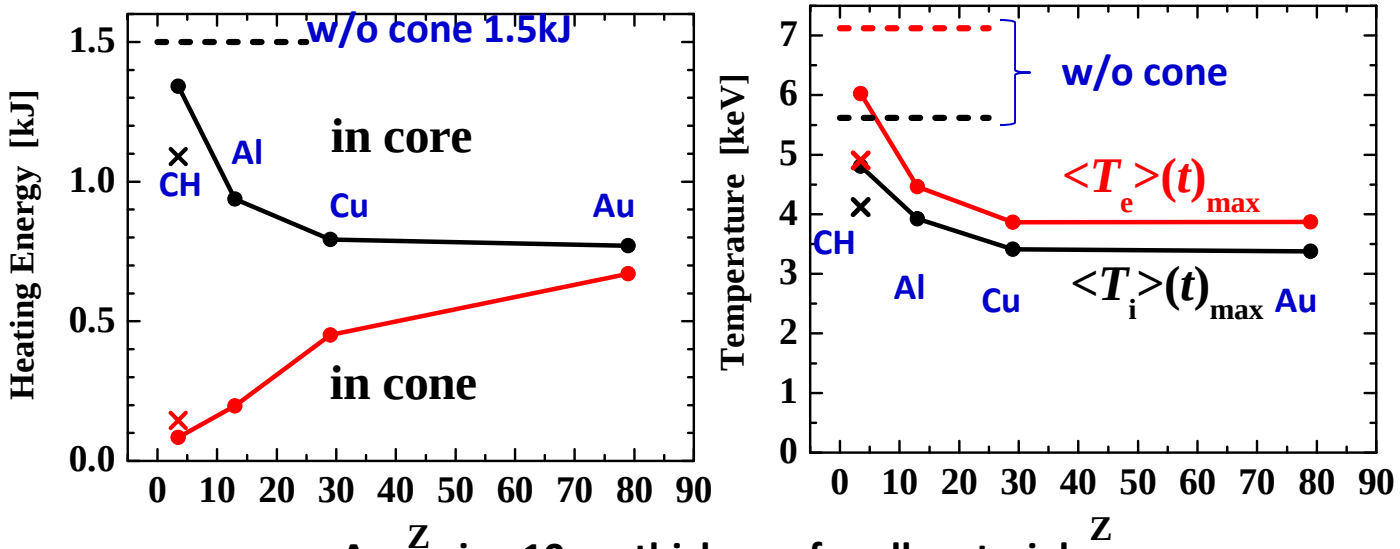

Assuming 10μm thickness for all materials
(x → CH cone 40um thickness)

Low-Z material is preferable for the cone tip material in perspective of generation and transport of fast electron because of the less collisional effects in cone tip.

Effect of Cone Tip Deformation

Fast electron heating rate [W/m^3] (B-field effects)

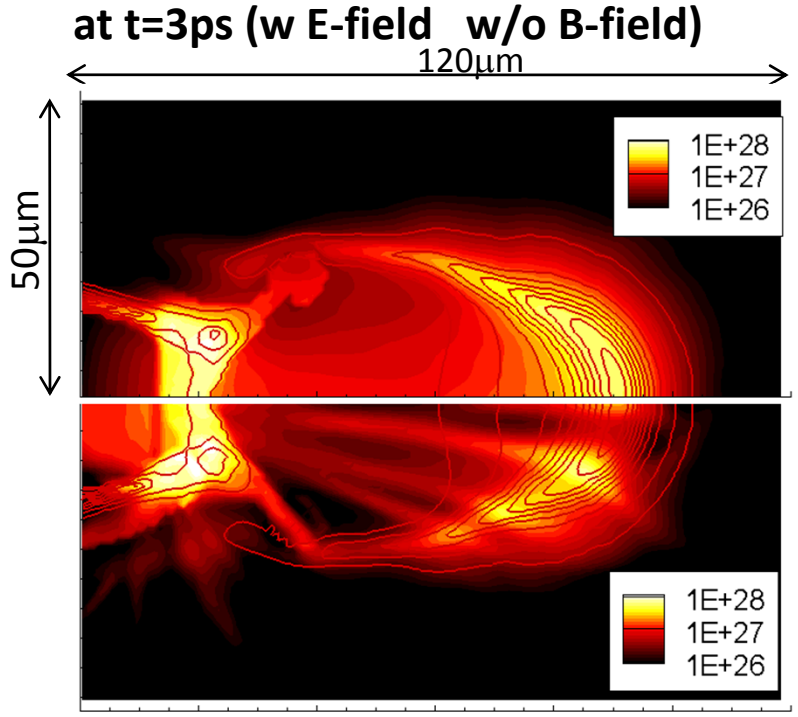

w/o B-field case

- collisional process (scattering and drag) in the Au cone tip reduce core heating rate

W B-field case

- In addition to the collisional effects, the fast electrons are scattered and trapped in the cone by the B-field generated around the cone tip, and the core heating rate decreases further!

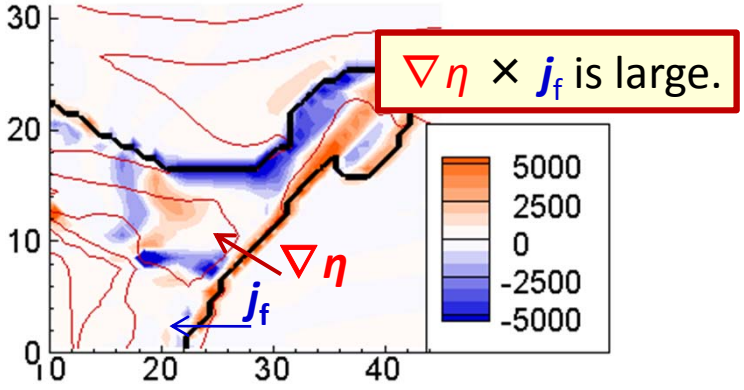

B-fields	$E_{dep,core}$ ($h_{fe->core}$)	$<T_e>_{DD,max}$	$<T_i>_{DD,max}$
w/o	1.83kJ (36.6%)	4.63keV	3.70 keV
with	1.04kJ (20.8%)	4.15 keV	3.24 keV

Effect of Cone Tip Deformation

(2D ALE-CIP Radiation-Hydro code, H. Nagatomo, ILE)

PINOCO

- 2 temperature plasma
  - Hydro ALE-CIP method
- Thermal transport
  - flux limited type Spitzer-Harm
  - Implicit (9 point-ILUBCG)
- Radiation transport
  - multi-group diffusion approximation
  - Implicit (9 point-ILUBCG)
  - Opacity, Emissivity (LTE, CRE)
- Laser energy
  - 1-D ray-trace
- EOS
  - Tomas-Fermi
  - Cowan

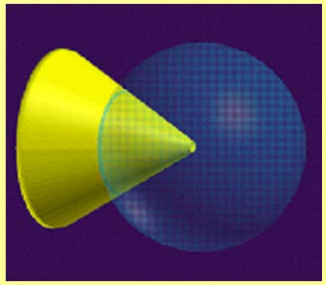

Implosion Laser condition

Gaussian pulse shaping

Wavelength : 0.53μm

Energy (on target) : 2.5 kJ

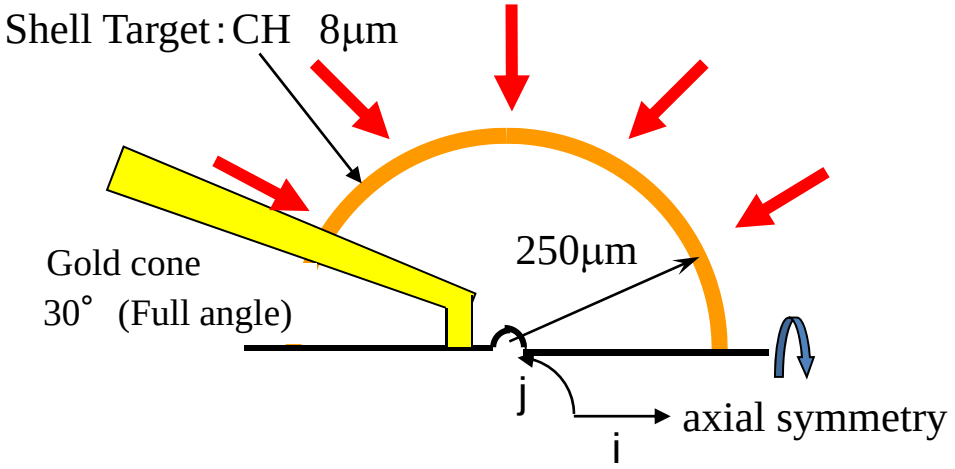

computational grids : 280 (i- dir.)x280 (j – dir.)

Effect of Cone Tip Deformation
FP Transport + Rad. Hydro

Core plasma・・・Rad. Hydro

Implosion simulation results for a CD shell + Au cone target (1.97ns, 50ps before max. compression)

ρ_{min} between cone and core = 1.5g/cm³

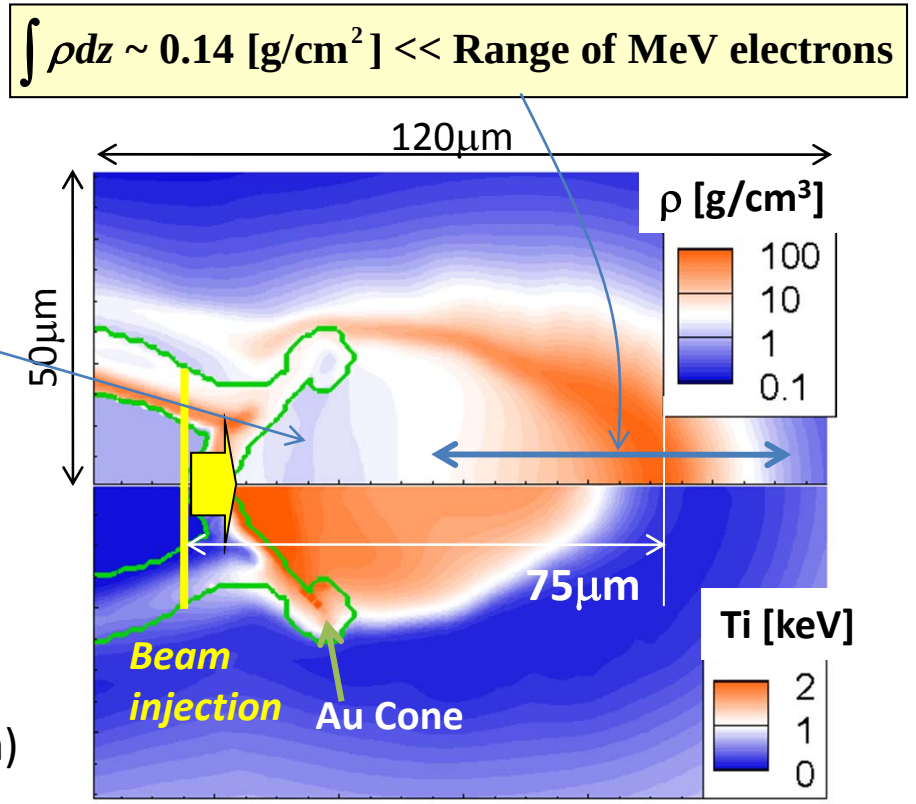

Fast electron・・・FP Transport

Injection point is 75μm away from the ρ_max

Super Gaussian, r_{HWHM} = 15μm in r-direction

E_{fe} = 5kJ (50% coupling of LFEX to fast electron)

T_{fe} 1.0MeV (slop temperature)

τ_{fe} = 5 ps

P_{fe} = E_{fe} / τ_{fe} = 1.0 (5ps) PW

I_{fe} = 1.4x10^{20}W/cm^2 at the central axis

Effect of Cone Tip Deformation

B-field around the "deformed" cone tip

$\nabla\eta \times j_f$ is large when the cone tip deformed!

Case 4 at 3ps; B-field [T]

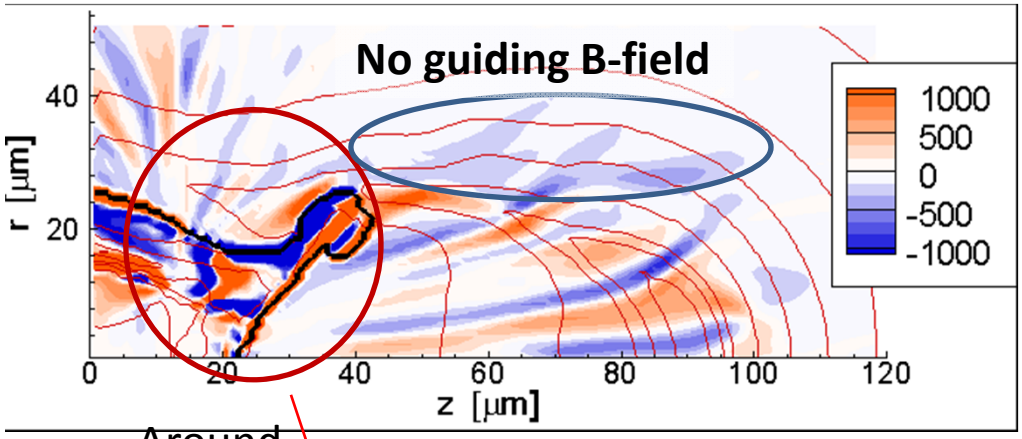

Around cone

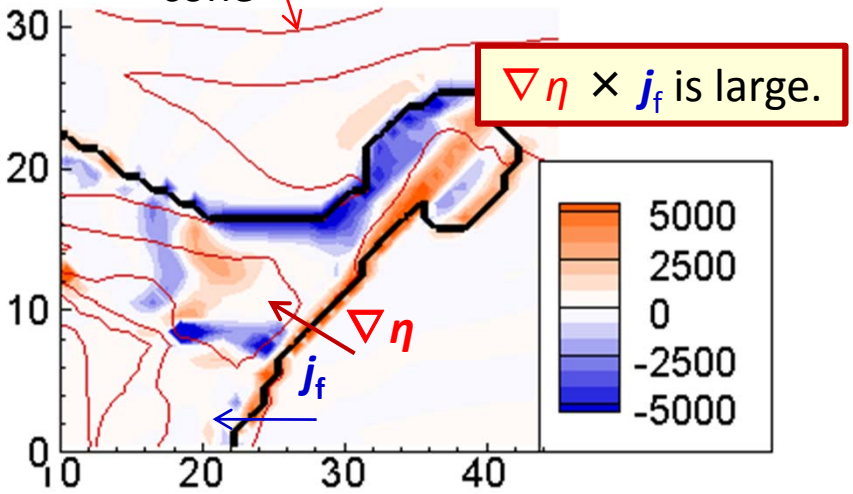

Spherical core + clean cone tip

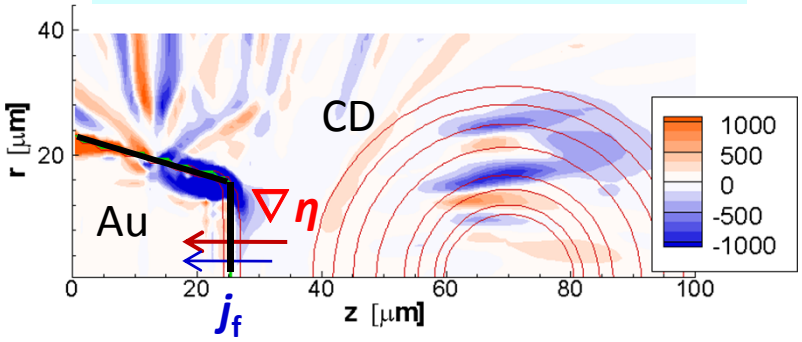

$\nabla\eta$ is large, but $\nabla\eta \times j_f$ is small.

- **Huge B-field is generated at the contact surface between "deformed" cone tip and imploded CD plasma due to $\nabla\eta \times j_f$, which strongly scatters and traps the fast electrons.**
- **Due to the large beam divergence after propagation in the cone, self-guiding resistive field is not formed.**

→ Reduction in core heating efficiency.

Effect of Cone Tip Deformation

Beam profile

Beam Power (r < 20μm)

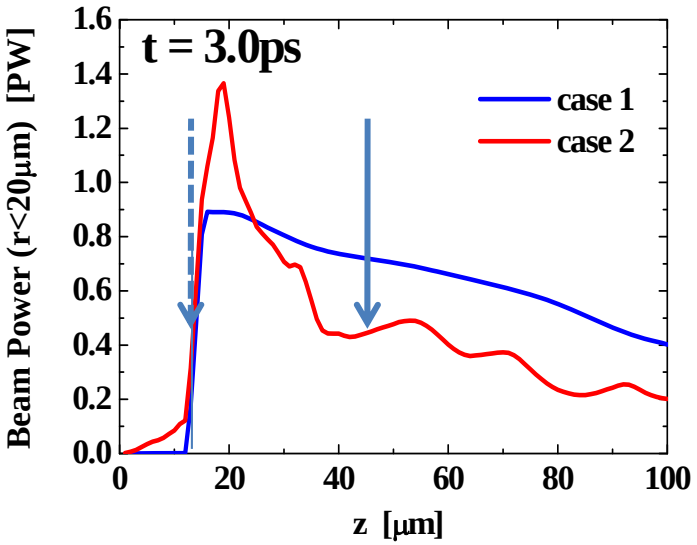

Angular distribution (r < 20μm)

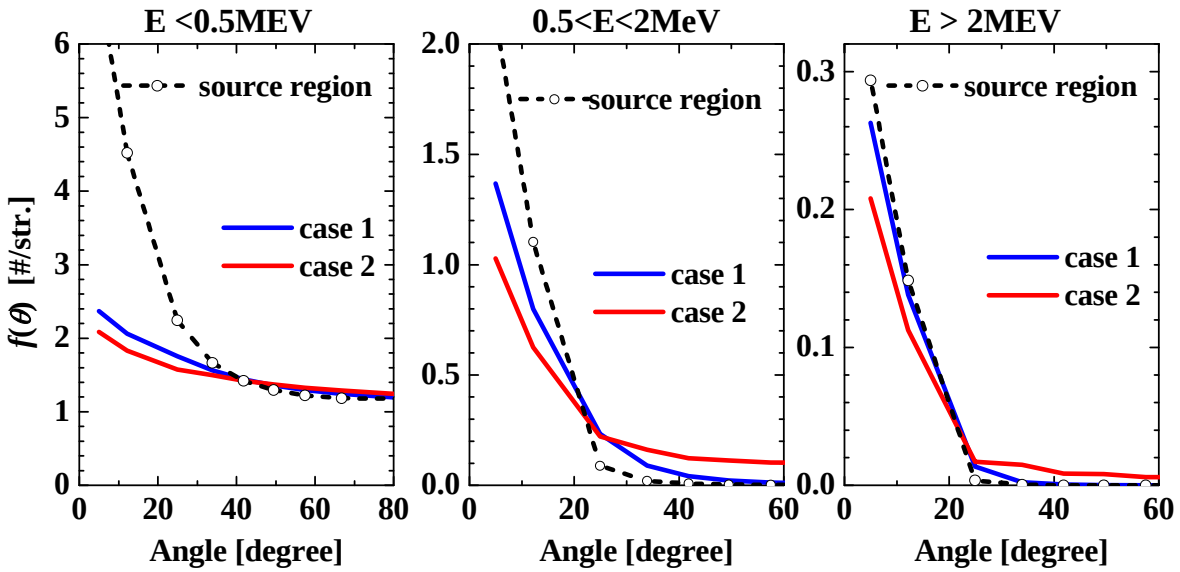

	collision	E-field	B-field
Case 1	on	on	off
Case 2	on	on	on

Because of the scattering & trapping due to B-field at the contact surface between "deformed" cone tip and imploded CD plasma, the 30% of the beam power is lost and the angular spread becomes large.

Effect of Cone Tip Deformation

Fast electron heating rate [W/m^3] (B-field effects)

at t=3ps (w E-field w/o B-field)

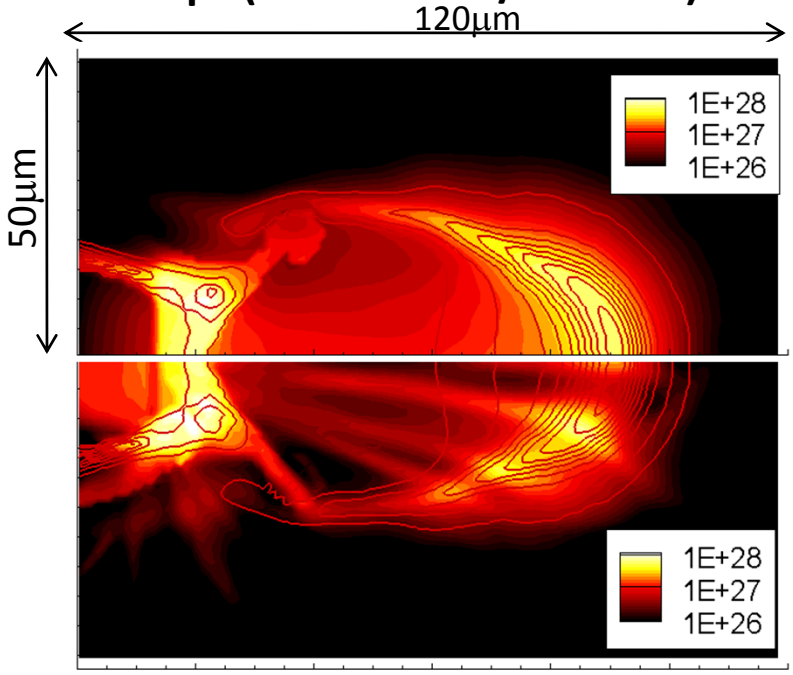

w/o B-field case

- **collisional process (scattering and drag) in the Au cone tip reduce core heating rate**

W B-field case

- **In addition to the collisional effects, the fast electrons are scattered and trapped in the cone by the B-field generated around the cone tip, and the core heating rate decreases further!**

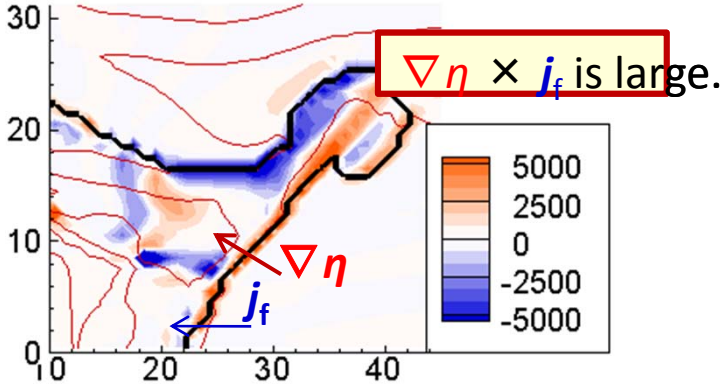

$\nabla\eta \times j_f$ is large.

B-fields	$E_{dep,core}$ ($h_{fe->core}$)	$<T_e>_{DD,max}$	$<T_i>_{DD,max}$
w/o	1.83kJ (36.6%)	4.63keV	3.70 keV
with	1.04kJ (20.8%)	4.15 keV	3.24 keV

3. Pre-plasma Effects

FIW2010, APS2010, IAEA Proc.
http://www-pub.iaea.org/MTCD/Meetings/PDFplus/2010/cn180/cn180_papers/ife_p6-01.pdf

Introduction

IAEA2010, FIW2010, APS2010

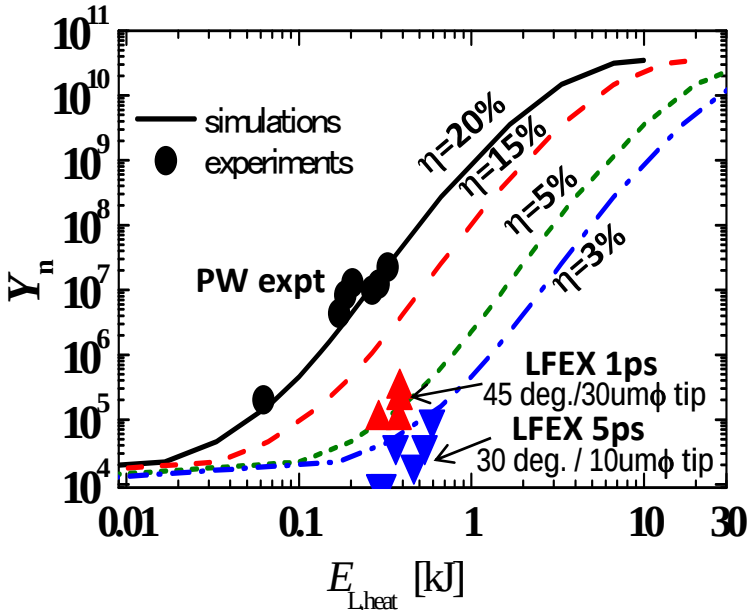

At the first integrated experiments (2009) using LFEX laser (0.3~0.8kJ/1~5ps), the neutron enhancement due to external heating is significantly lower than that obtained at the GX-II+PW laser system (2002).

The reduction of neutron enhancements may be due to the pre-plasma generated in the cone by low-intensity pre-pulse of heating laser.

- **Increasing electron energy**
- **pulling the generation point away from the tip**

→ These will reduce the energy coupling efficiency for heating laser to core.

Evaluation by 2D PIC + FP simulations

- **Pre-plasma effects on core heating in cone-guiding fast ignition**
- **New concept "extended double cone" for improving core heating performance**

http://www-pub.iaea.org/MTCD/Meetings/PDFplus/2010/cn180/cn180_papers/ife_p6-01.pdf

2D PIC simulation condition (collisonless)

Fast electron observation point (15um width)

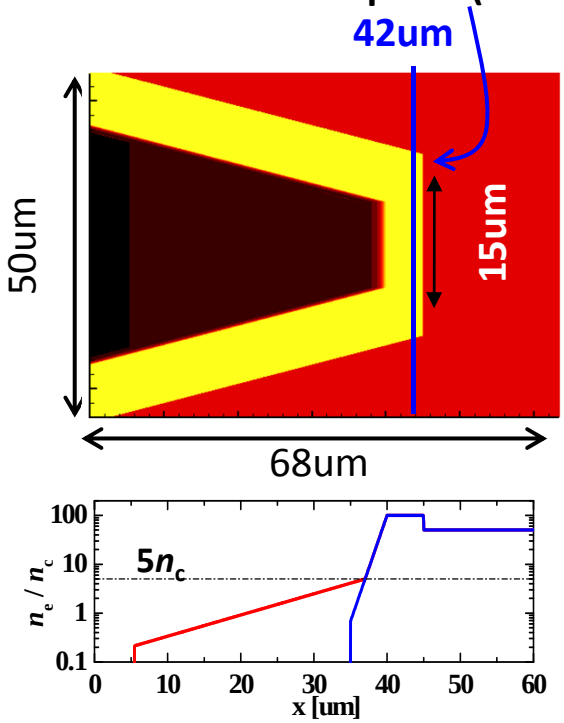

- run
  - Total run time: 450 τ_L (~1.6 ps)
  - 68λ x 50λ
  - 64 cells per wavelength
  - 24~48 electrons (or ions) / cell.
  - MPI: 128 CPUs (200~380GB & 120 hrs)
  - Domain width is dynamically adjusted to make sure that each domain has the same number of particles.

2D PIC code "ASCENT", H.-B. Cai

- ***Cone; single/double/extended double***

Full angle	30 deg.
Cone tip width (inner)	**$12\lambda_L$**
Cone wall width	$8\lambda_L$
Material	Au with Z = 40
Electron density	$100n_c$
Pre-plasma scale	$1\lambda_L$ ($>5n_c$) **+ $10\lambda_L$ ($<5n_c$)**
Outer region	$50n_c$ CD plasma

Double cone case
(inner wall 3umt, gap 3umt, outer wall 2umt)
Extension length 20um

- ***Laser***

$<I_L>$ = 3×10^{19}W/cm^2 ($<a>$ =4.7)
Temporal profile: 1ps flat pulse
Gaussian ramp ($\tau_{rise} = 10T_0$) - Constant ($\tau_L = 300T_0$) – Gaussian damp ($\tau_{damp} = 10T_0$)
Spatial profile:
Gaussian with $\phi_L = 16.5\lambda_L$ (FWHM)
focus point x = 0 & y= 0
Input Energy : 4.37J/um

- ***Boundary***

✓**Fields:** absorbing in both x and y boundary
✓**Particles:** absorb ions at both boundaries, electrons only if charged at both x and y directions. The Artificial damping for fast particles at the boundary are introduced.

- ***Weighted particle method***

Pre-Plasma effects for laser-cone interactions 1

w/o pre-plasma

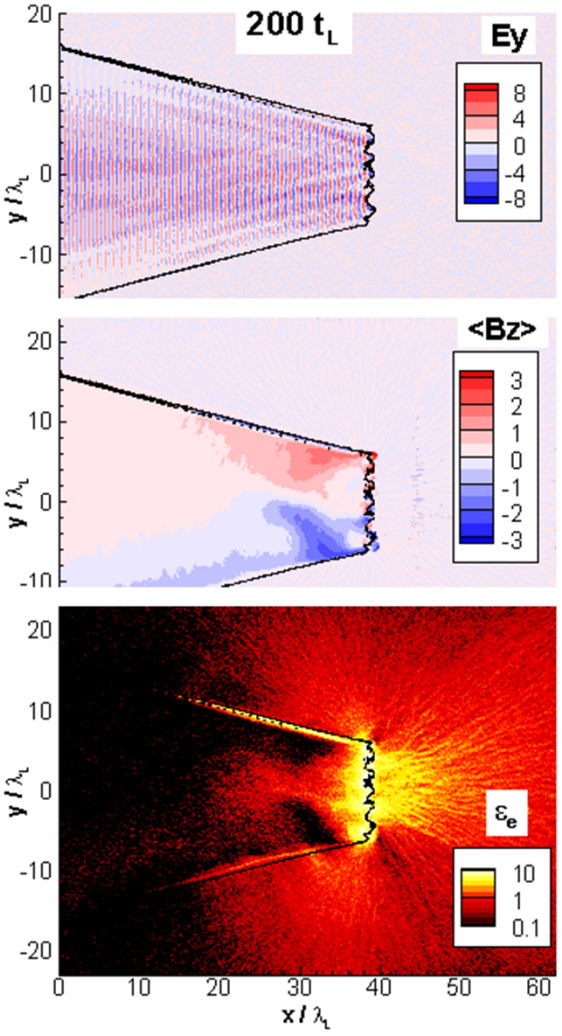

with pre-plasma

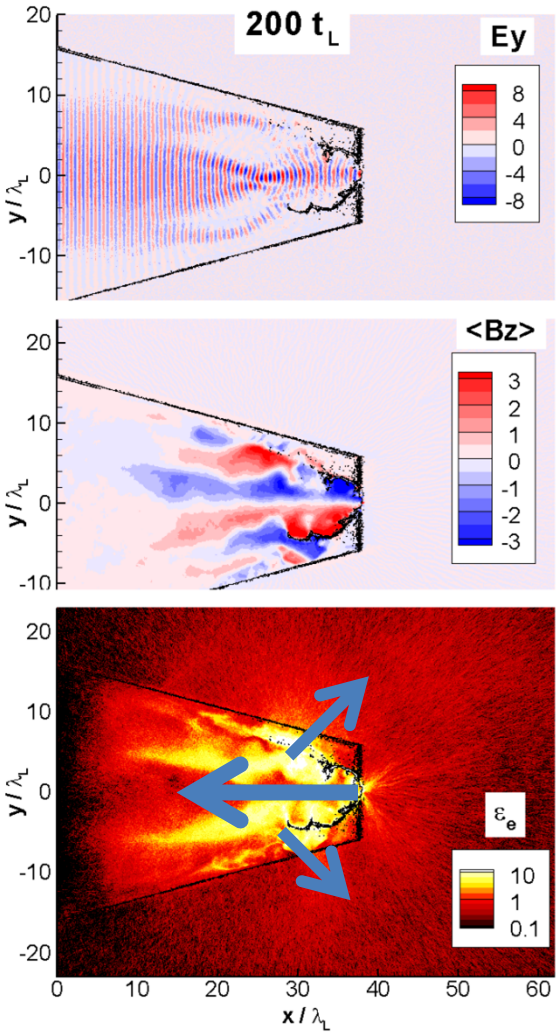

Phase plot at 200 τ_L

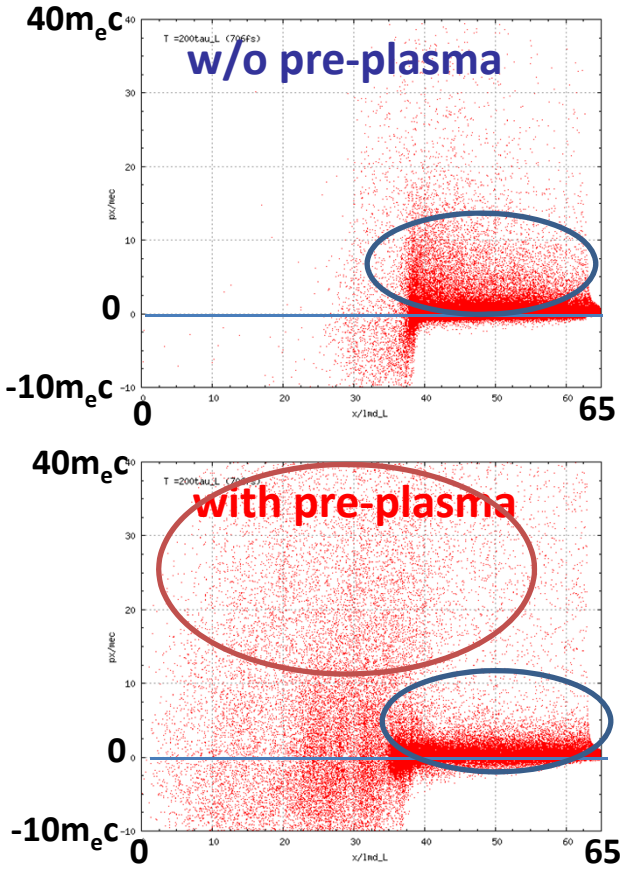

Pre-Plasma effects for laser-cone interactions 2

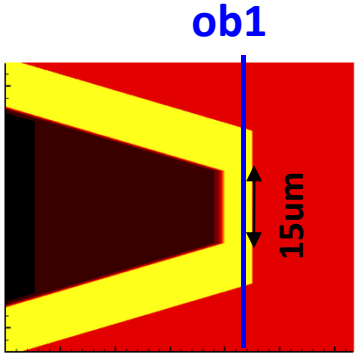

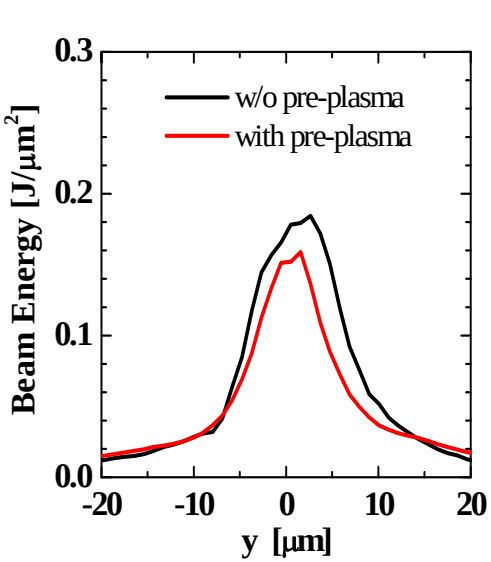

Integrated over time in 15um width region

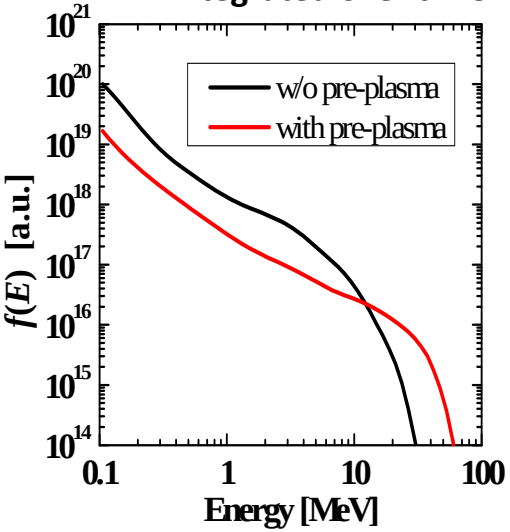

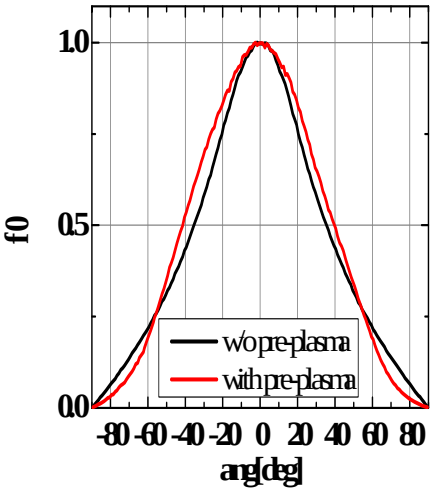

	w/o pre-plasma	with pre-plasma	ratio
E-beam energy*	**2.05J/um (48%#)**	**1.57J/um (36%#)**	**24% ↓**
Fraction			
E < 2 MeV	0.56 (13%#)	0.12 (3%#)	**78% ↓**
E = 2~10MeV	1.16 (26%#)	0.34 (8%#)	**71% ↓**
E > 10 MeV	0.34 (8%#)	1.10 (25%#)	**230% ↑**

* Observed at end of tip ($x = 42\lambda_L$) in the region of ($-7.5\lambda_L < y < 7.5\lambda_L$)

\# Energy coupling of laser to E-beam up to 1.6ps.

PIC results → Core Heating sim. (FP simulations)

PIC Simulations; e^- beam generation

- ***Cone; single/double/extended double***

Full angle	30 deg.
Cone tip width (inner)	**$12\lambda_L$**
Extension length	20um

- ***Laser***

$<I_L>$ =	**3 x10^{19}W/cm^2 ($<a>$ =4.7)**
Temporal profile:	**1ps flat pulse**
Spatial profile:	
Gaussian with	**$\phi_L = 16.5\lambda_L$ (FWHM)**
focus point	x = 0 & y= 0
Input Energy E_L :	4.37J/um

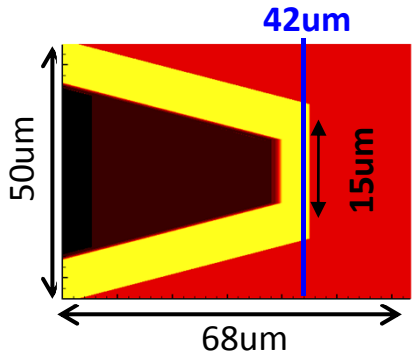

For cylindrical geo., *E*L = 92.5J
(much less than LFEX 2beam 2kJ because of small spot & short duration)

Experiments

- ***Cone;***

Cone tip width inner (outer) 40umϕ (50um ϕ)
(about 3.3 times larger than PIC)

FP Simulations; transport & heating

- ***e^- beam***

Using PIC results $f_e(p, \mu, \omega, y, t)$
 # beam spot is extended x3.3 from PIC results.
15umϕ observation in PIC -> 50umϕ input in FP
(Corresponding laser energy ~1kJ for cylindrical)

- ***CD core***

Gaussian; 100g/cm^3 peak, 28umϕ, 0.15g/cm^2
Uniform temp 0.3keV

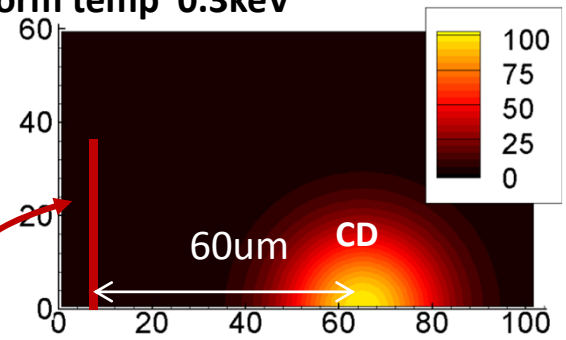

Fast electron profiles evaluated in 2D PIC simulations are used as the Fast electron beam source if FP sim. For core heating.

2D FP-Hydro code "FIBMET", T. Johzaki

Core Heating Sim (PIC&FP results)

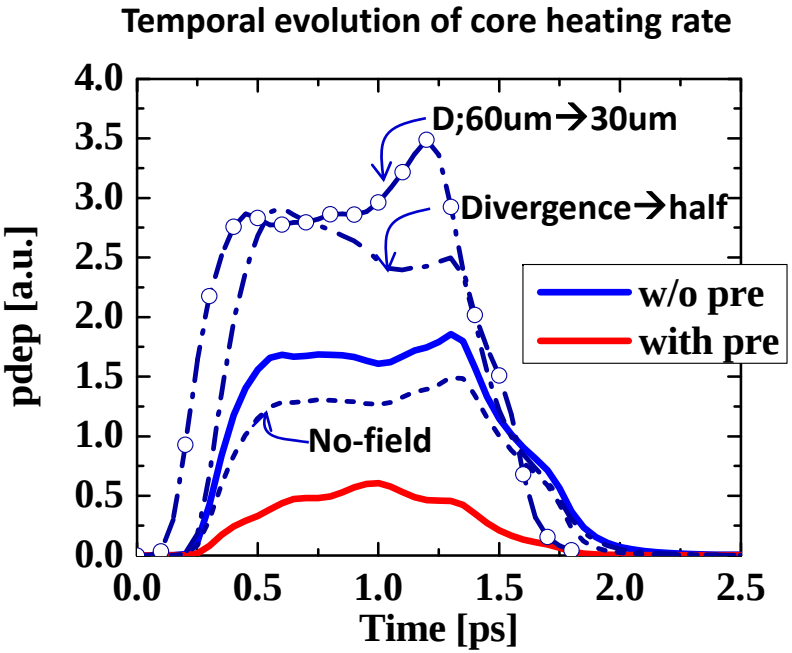

- **Decreases in number of relatively low energy fast electrons due to pre-plasma considerably reduces the heating rate.**
- Due to large beam divergence & low beam intensity, collimation field ($\eta \nabla \times j_f$) is not so strong.
  → Beam collimation due to resistive field is not remarkable.

To enhance the core heating efficiency,

1. making beam divergence smaller at generation
2. putting tip close to the core
3. guiding beam close to the core

Pre-plasma	dist	field	θ_{beam}	$\eta_{L\rightarrow fe}$ [%]	$\eta_{fe\rightarrow core}$ [%]	$\eta_{L\rightarrow core}$ [%]	$<Ti>_{DD}$[keV]	Yn_{DD}
w/o	60	on	PIC	48	16	7.5	0.75	1.2e6
with	60	on	PIC	36 (24%↓)	4.7(71%↓)	1.7(78%↓)	0.35	8.7e4
w/o	60	off	PIC	48	12 (23%↓)	5.8(23%↓)	0.47	3.5e5
w/o	60	on	½ PIC	48	25 (57%↑)	12 (57%↑)	0.77	2.0e6
w/o	30	on	PIC	48	29 (80%↑)	14 (80%↑)	0.85	3.6e6

The Values in () are the ratio to the case w/o pre-plasma (first line).

4. Extended Double Cone

FIW2010, APS2010, IAEA Proc.
http://www-pub.iaea.org/MTCD/Meetings/PDFplus/2010/cn180/cn180_papers/ife_p6-01.pdf

New Concept; Extended Double Cone

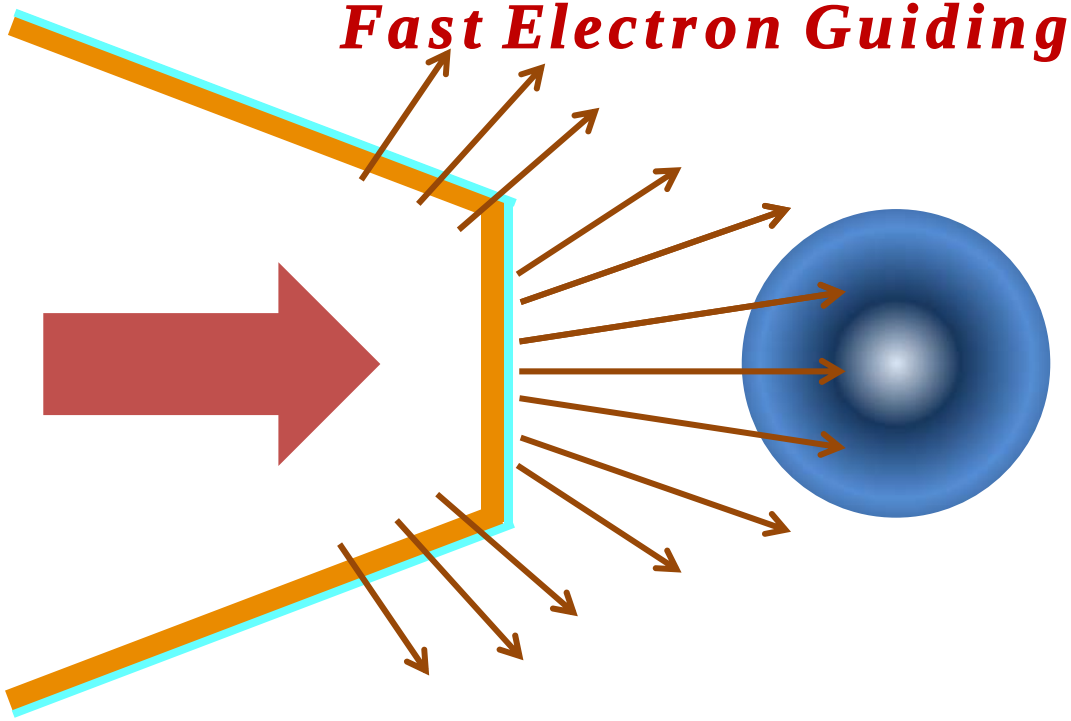

In the single cone case, fast electrons generated at the cone wall freely escape.

New Concept; Extended Double Cone

Fast Electron Guiding & Focusing

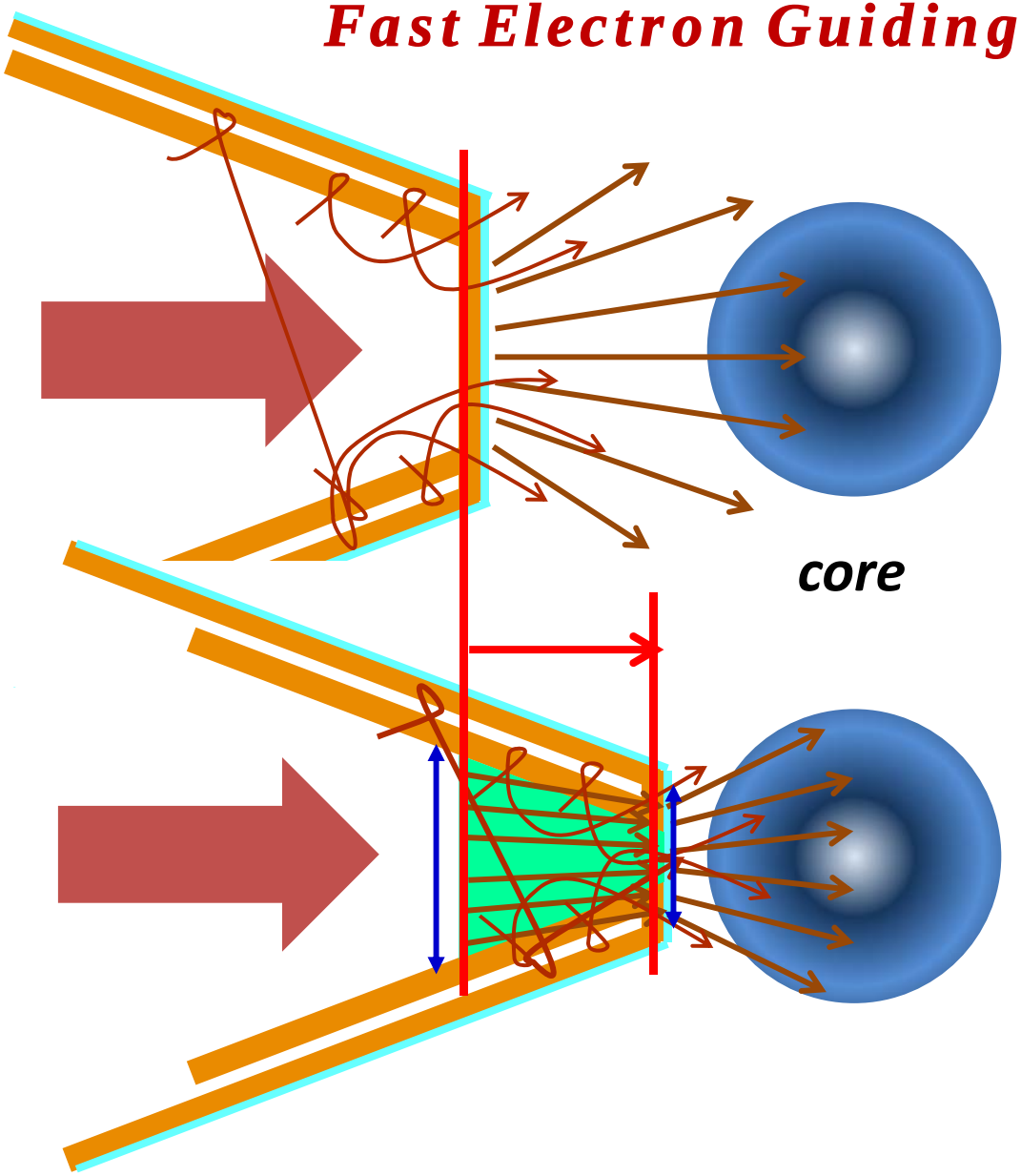

Using double cone, fast electrons confinement due to B-field can be expected. But, the beam divergence is large and several tens of microns of distance remains from tip to core.

→ Even using double cone, some of beam loss due to beam diverging occurs.

"Extended double cone" for beam guiding to core & focusing.

B-fields generated in extended vacuum gap region confine the fast electrons and then

1. beam guiding to the core is expected.
2. by changing the "open gate" (distance between the gaps at end of tip), the beam spot can be controlled.

Fast electron Guiding & Focusing by Extended Double Cone

Fast electron energy density (100keV < E < 5MeV)

Single cone

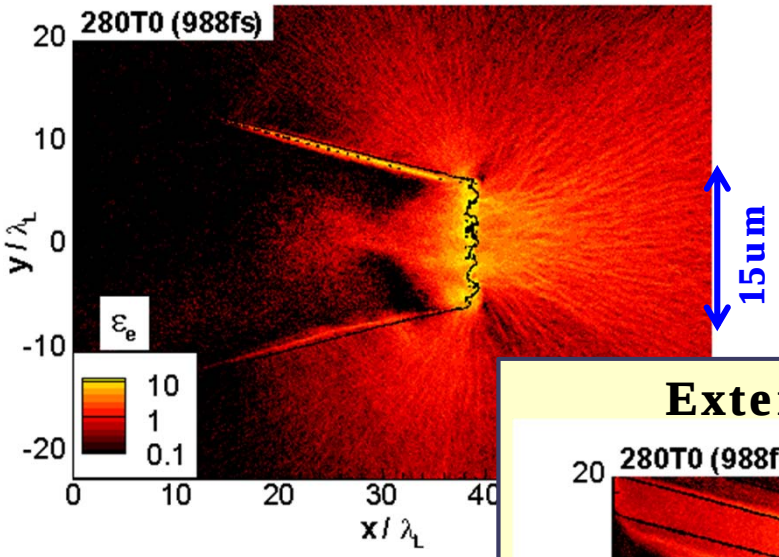

Double cone

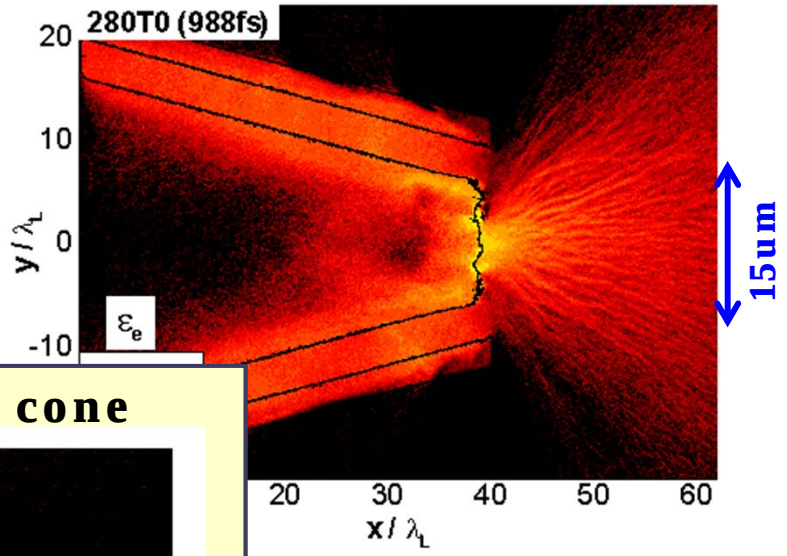

Extended double cone

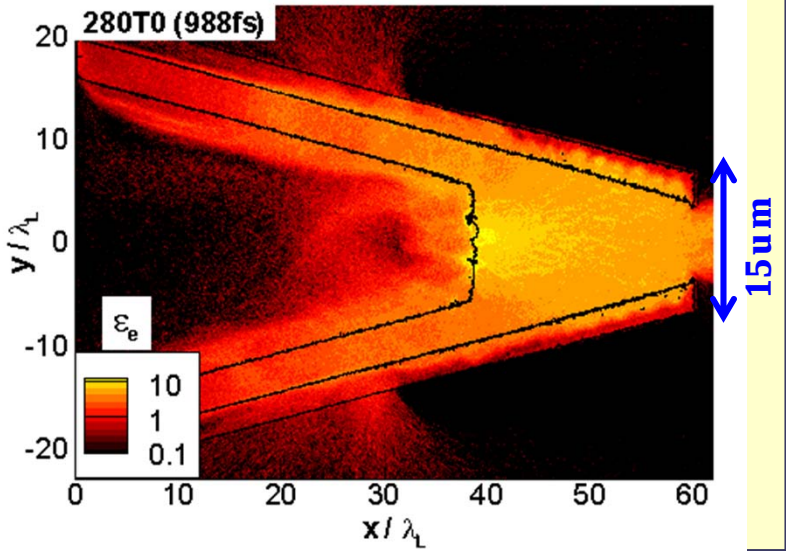

Extended Double Cone; Beam profiles

Fast Electron Guiding & Focusing

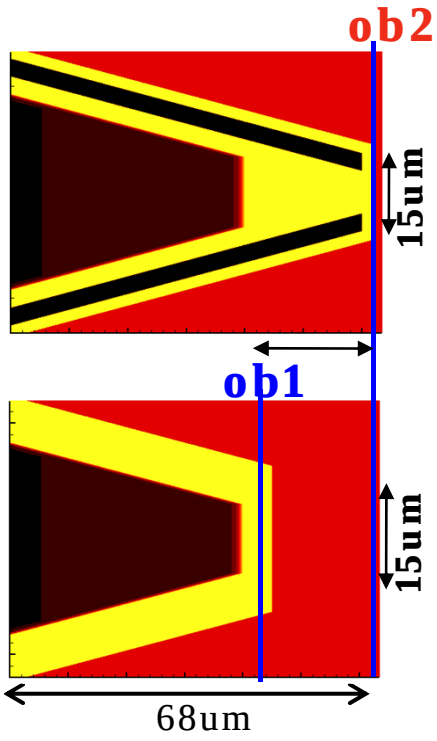

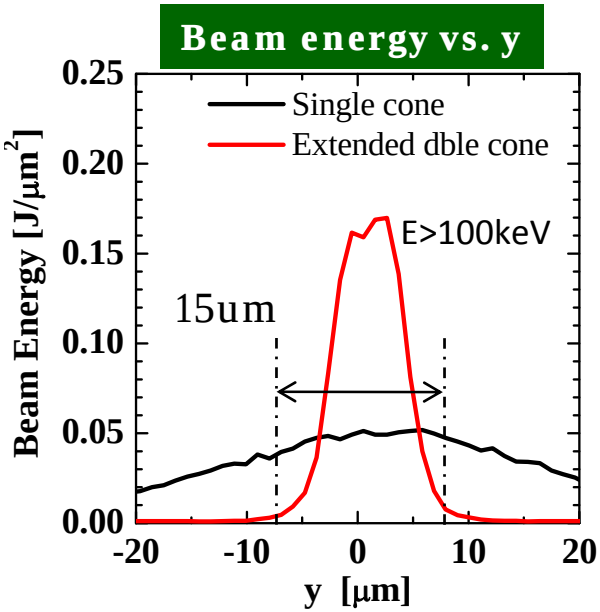

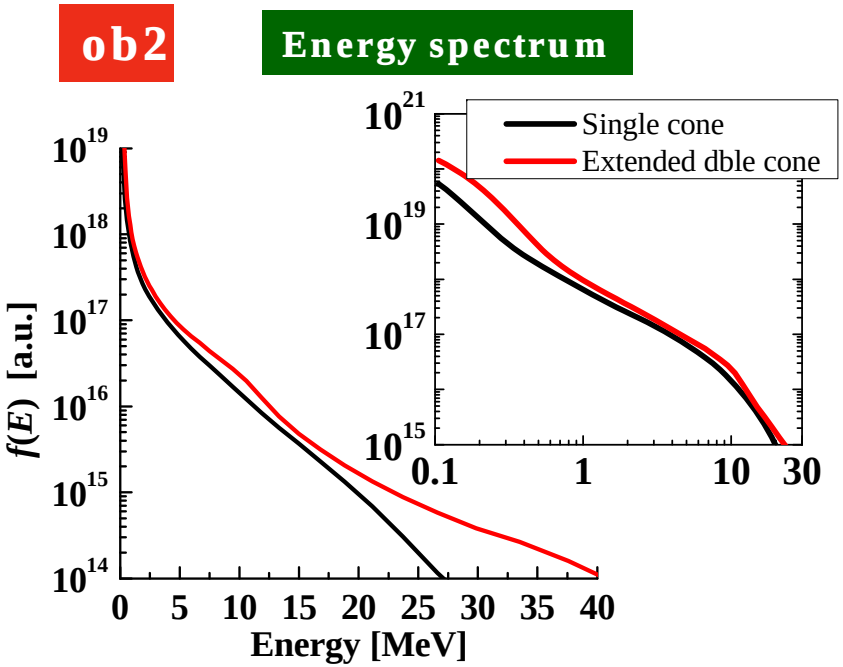

Core Heating simulation
Fokker-Planck with PIC source

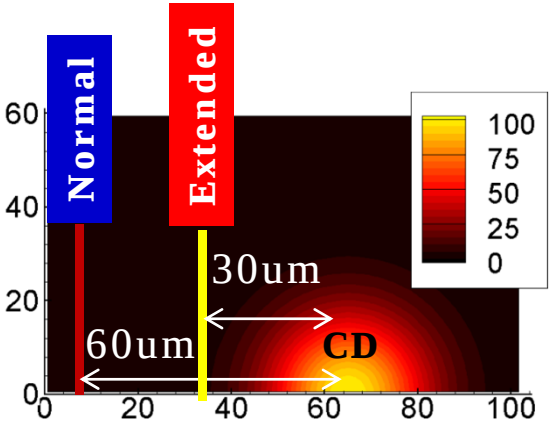

Summary 1

Fast Electron Guiding & Focusing

Pre-plasma dist		$\eta_{L\rightarrow fe}$ [%]		$\eta_{fe\rightarrow core}$ [%]	$\eta_{L\rightarrow core}$ [%]	<Ti>$_{DD}$[keV]	Yn$_{DD}$
Single		*x*=42um (62um)					
① w/o	60	48	(18)	16	7.5	0.75	1.2e6
② with	60	36	(14)	4.7	1.7	0.35	8.7e4
ratio to w/o					-71%	-78% -97%	
Extended double		*x*=62um					
❶ w/o	30	31		62	19 (+153%)	1.27 (+120%)	1.4e7
❷ with	30	20		28	5.5(+224%)	0.70 (+3800%)	4.0e5
ratio to single w/o pre					-27%	-7%	

The Values in () are the ratio to the single cone cases

- ■ Comparison between ① and ❶ / ② and ❷.
  - ➢ The extended double cone effectively enhances the fast electrons with energy of E<10MeV which mainly contribute to core heating, regardless of pre-plasma.
- □ Comparison between ① and ❷.
  - ➢ Even if the extended double cone is used for the case with pre-plasma, however, the negative effects of pre-plasma (reduction of $\eta_{L\rightarrow core}$) can not be overcome.
  - ➢ The beam transverse profile is more peaky for the extended double cone case. Thus, the heating region is narrower and core temperature becomes locally higher for ❷ than ① even for the lower total coupling $\eta_{L\rightarrow core}$.

Advanced Concept of High-Energy Coupling Cone for FIREX-I

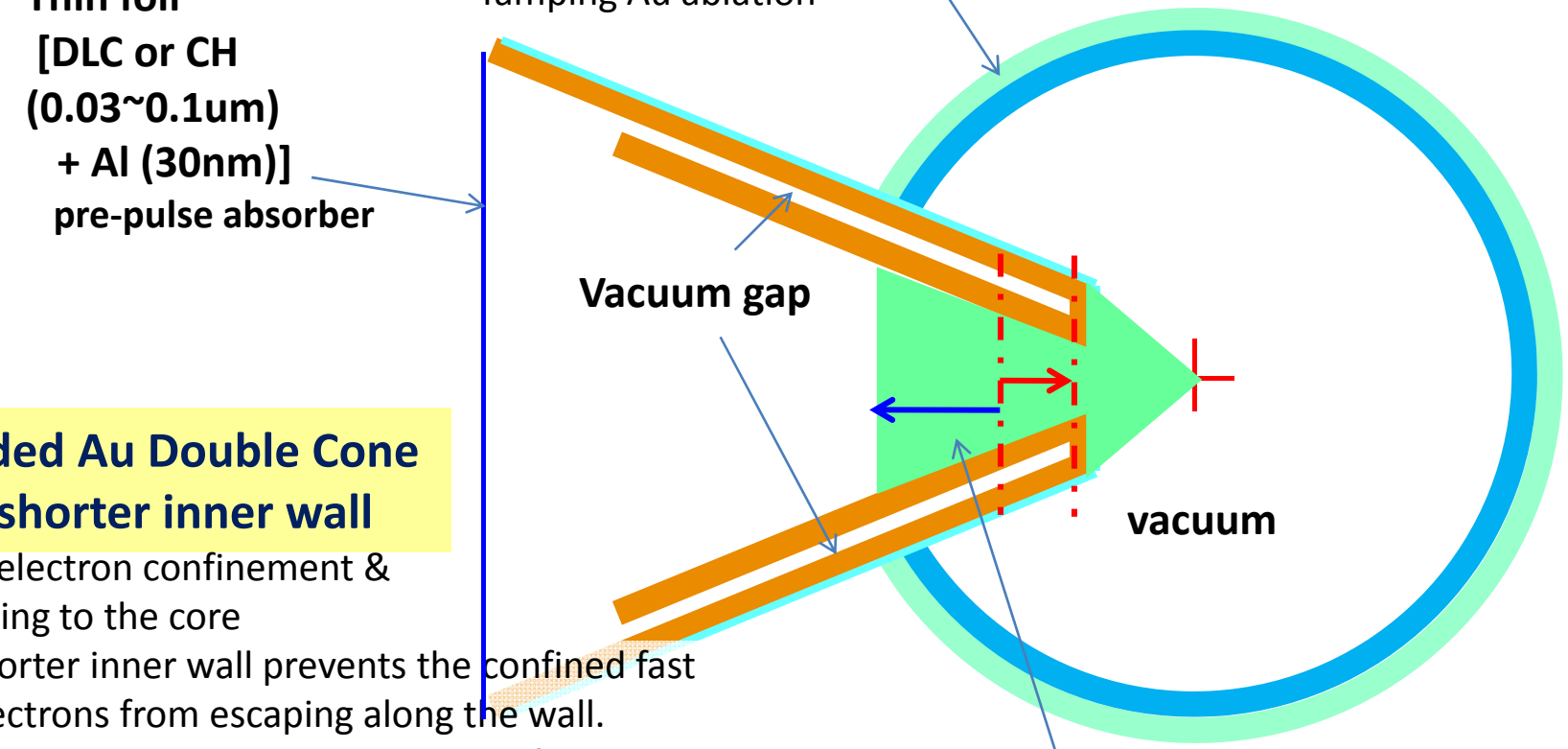

Extended Au Double Cone with shorter inner wall

Fast electron confinement & guiding to the core

1. Shorter inner wall prevents the confined fast electrons from escaping along the wall.
2. **Extended vacuum gap guided the fast electron close to the core.**
3. **A possibility to reduce the intensity and soften fast electron spectrum by pulling the tip surface away from the core to enlarge the interaction surface area.**

Low-Z "TONGARI" (pointed) tip

Low-Z …… lowering the collisional effects during long distance propagation

TONGRI… keeping the tip for a long time by letting plasma jet slip on the TONGARI surface

5. Resistive Guiding of Fast Electrons using Tongari (Pointed) cone tip

Preliminary results

Double cone (collisionless field)

|Bz| ~ 300MG

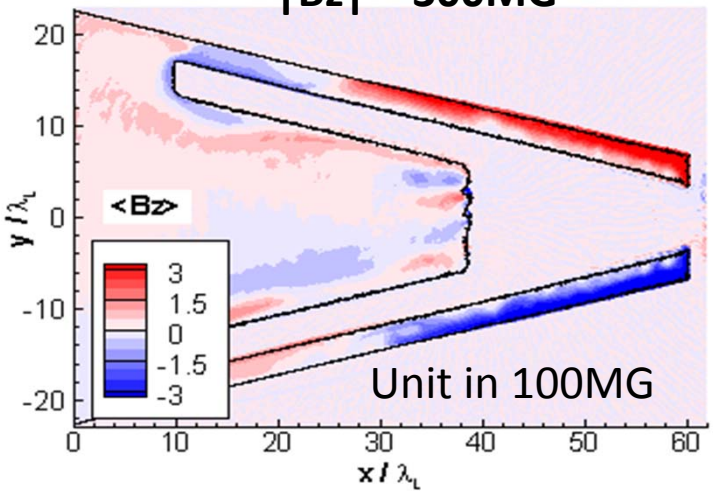

2D collisional PIC

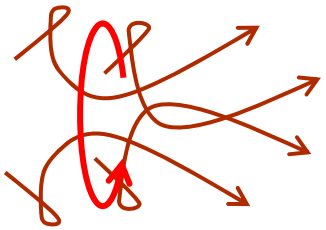

The direction of B-field is scattering one. But 300MG is strong enough to confine the electrons with E< 10MeV. So Confined fast electrons diffusively propagate toward the tip.

Single cone (resistive field)

|Bz| ~ a few tens of MG

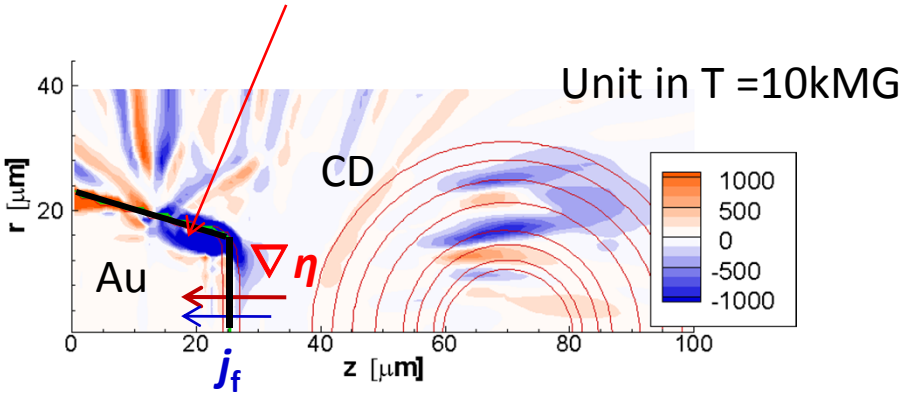

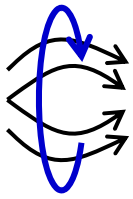

2D FP

The direction of B-field is opposite to that for double cone → Collimation B-field. But the strength is lower by 1 order of magnitude.

Which is better ??

Simulation Condition 1; plasma plofiles

Initial density profile

Au flat tip (19.7g/cm^3)

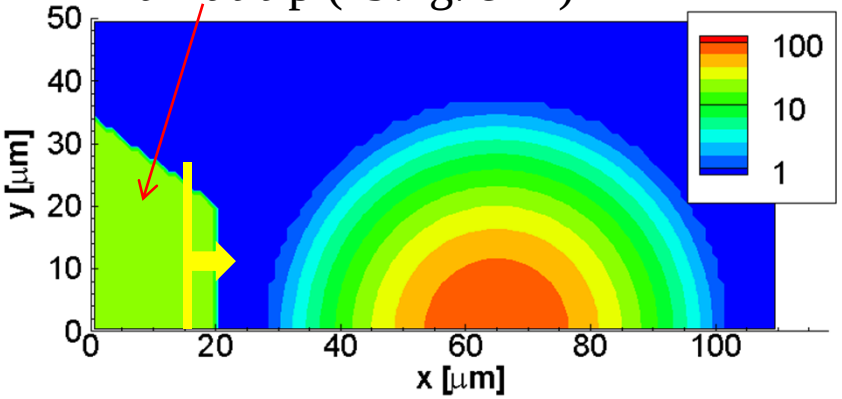

Tongari tip

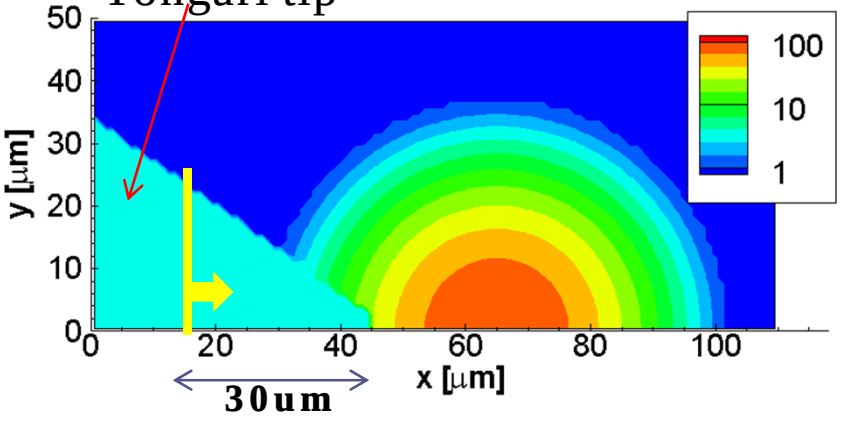

300eV uniform temp. (Te = Ti)

Normal cone (Au flat top)

transport thickness 5um

material	Z0	ρ	$n_e * d_t$ (full)
Au	79	19.3g/cm^3	2.32e21#/cm^2

Tongari cone

Angle 35^o

transport thickness, d_t 30um

top of tip width 6umf

material	Z_0	ρ	$n_e * d_t$ (full)
DLC	6	3.5g/cm^3	3.14e21#/cm^2
Al	13	2.7g/cm^3	2.34e21#/cm^2
Cu	29	9.0g/cm^3	7.38e21#/cm^2
Au	79	19.3g/cm^3	13.9e21#/cm^2

Simulation Condition 2; fast electron beam

Source profile from PIC sim.

- *Cone; single cone*
  - Full angle: 30 deg.
  - Cone tip width (inner): $12\lambda_L$
  - Material: Au with Z = 40
  - Electron density: $100n_c$
  - Pre-plasma scale: $1\lambda_L$
- *Laser*
  - $<I_L>$ = $3 \times 10^{19} W/cm^2$ ($<a>$ =4.7)
  - Temporal profile: 1ps flat pulse
  - Spatial : Gaussian , $\phi_L = 16.5\lambda_L$ (FWHM)
  - Input Energy : E_L= 4.37J/um

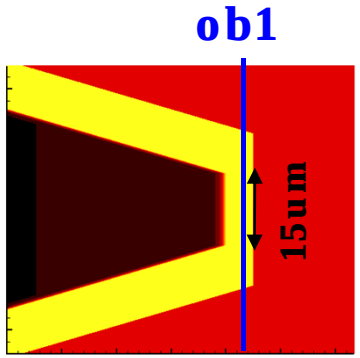

Fast electron profile observed at **ob1**

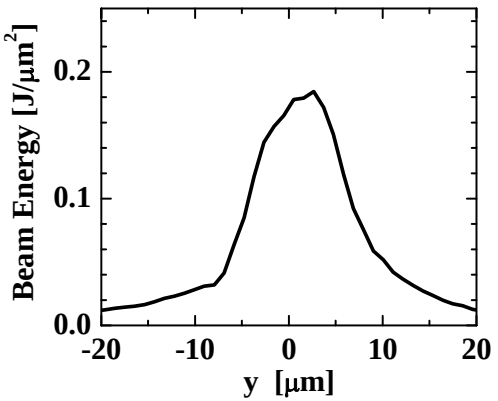

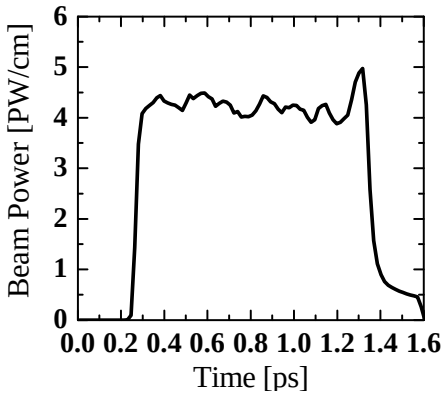

Integrated over time in 15um width region

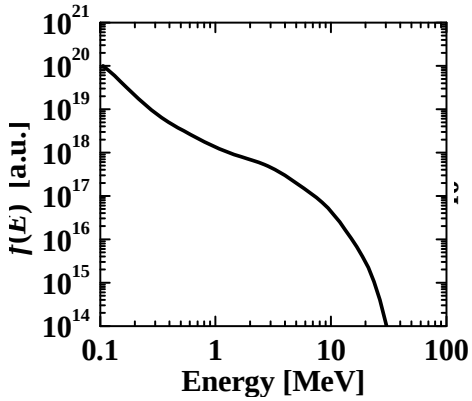

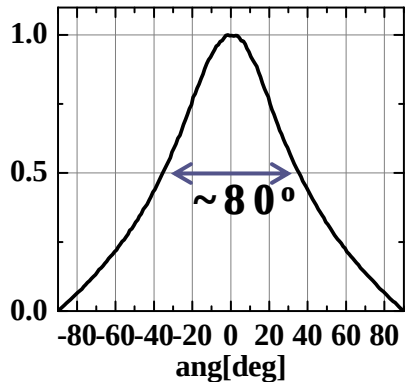

→ **In FP, beam spot is extended 3.3x from PIC results.**

Comparison between Au flat and DLC tongari

1ps

Au flat

DLC tongari

B_z [T]

p_{dep} [W/m^3]

T_e [keV]

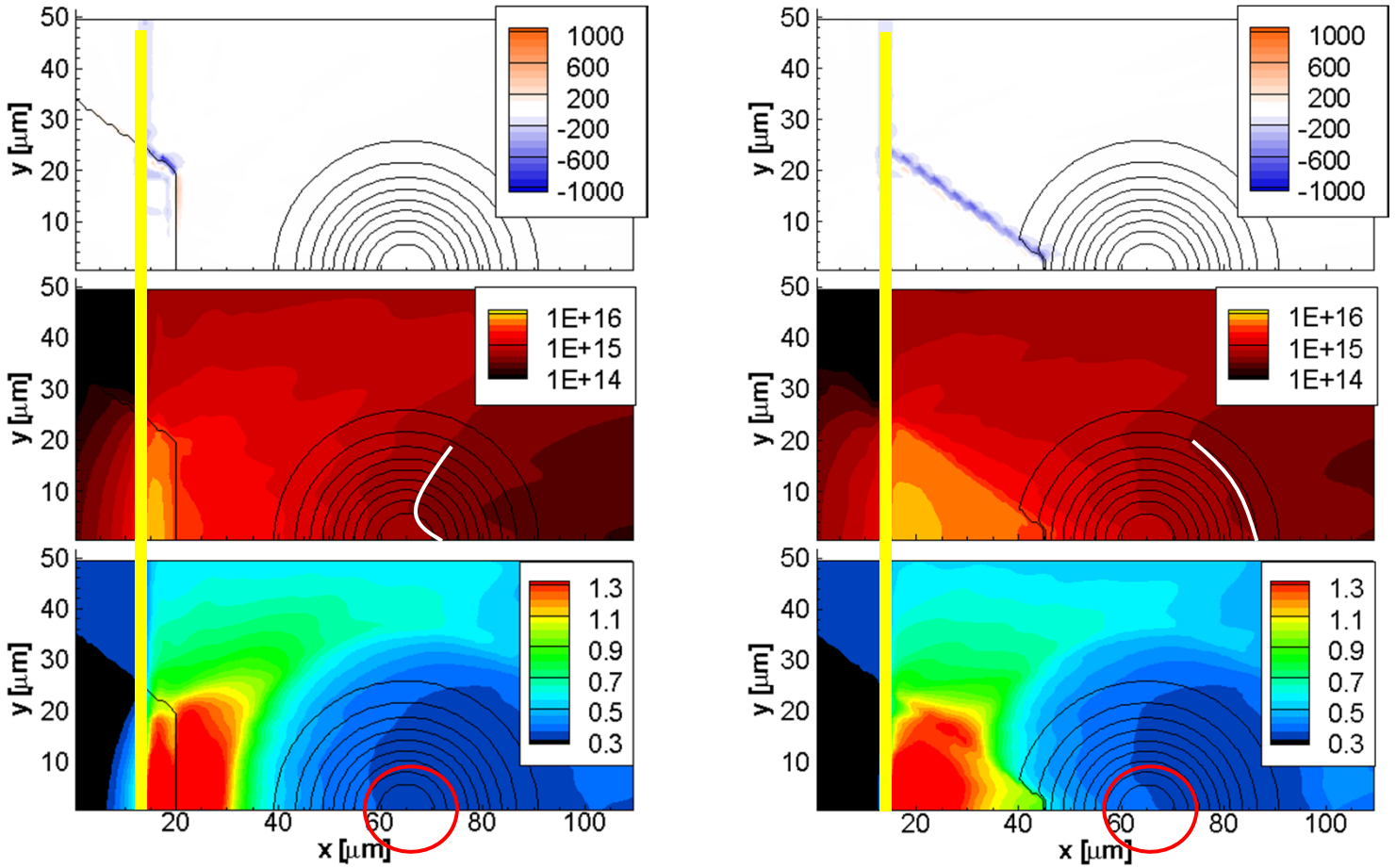

Material dependence

|B|max

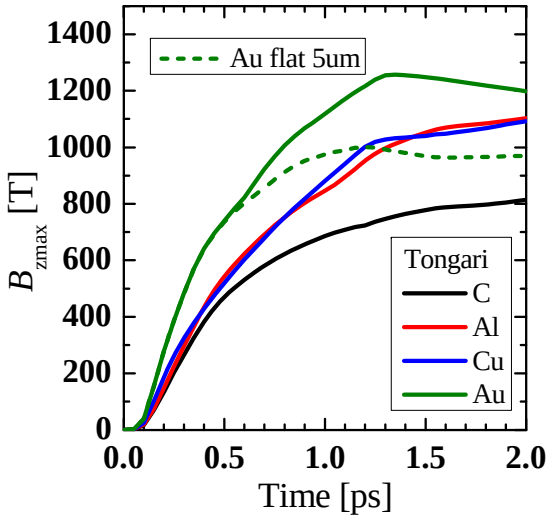

Heating power

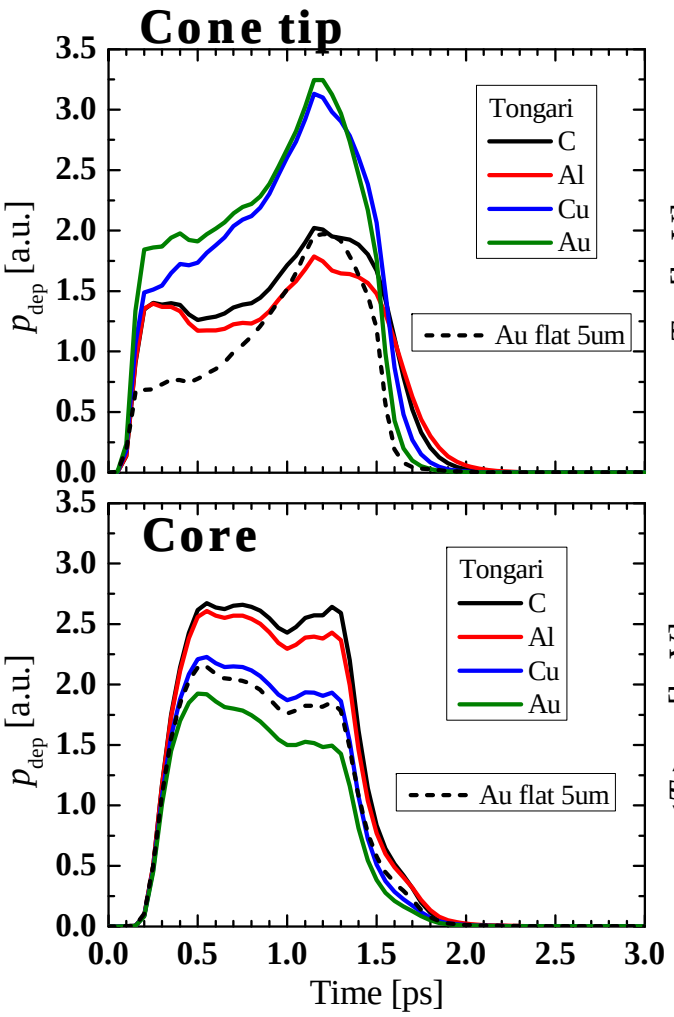

Core ele temp

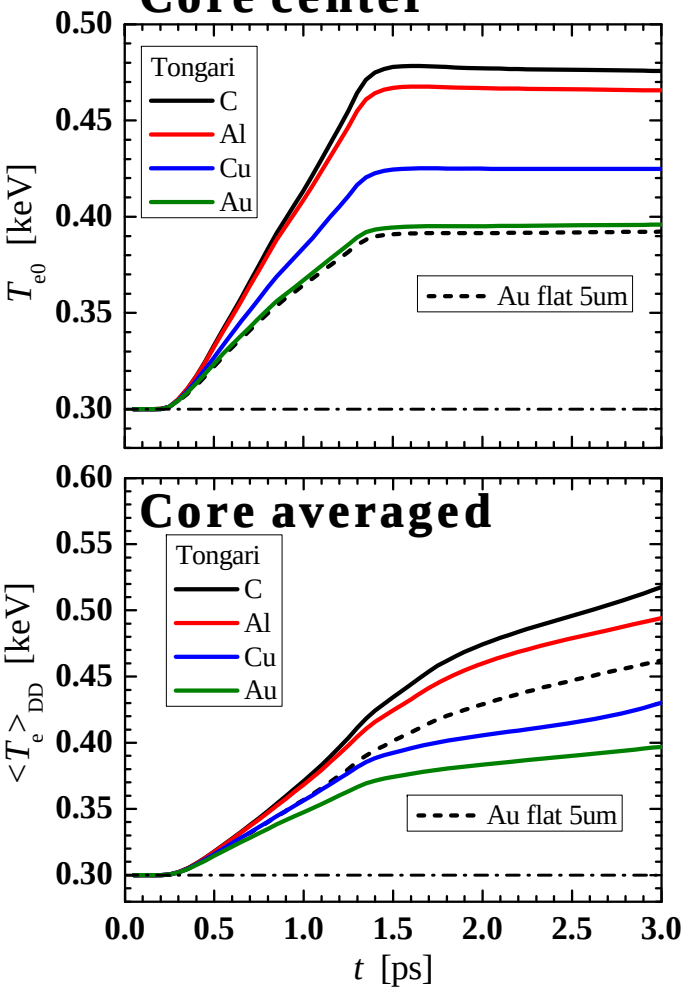

Summary

Tip	B_{max},	Econe*	*E*core*	ΔT_{e0} [keV]*
Au flat[5um]	999T	1	1	1
Au Tongari	1250T	1.9	0.8	1.0
Cu Tongati	1020T	1.8	1.0	1.4
Al Tongai	977T	1.3	1.3	1.8
DLC Tongari	723T	1.4	1.3	1.9

* normalized by the values for Au flat [5um] case

- ✓ **The resistive guiding using Tongari cone tip is effective if using low-Z material.**
  ***i.e.*, The energy coupling of fast electron to core is 30% higher and ΔT_{e0} is 90% higher for DLC tongari tip case.**
- ✓ **But using high-Z material, the energy loss in the long tip becomes larger, which results in lower energy coupling to core.**

Questions

- What's happen for deformed tip case due to the implosion?
- Can the tongari tip be used for ignition scale target?
- Which type of cone is more effective for core heating, Extended double cone or Tongari-single layerd cone?

Summary

- **Extended Double Cone**
  - **Due to the magnetic field at the gaps, the fast electron can be guided and focused, which enhances the core heating efficiency**
- **Tip Material Dependence**
  - **Low-Z material is (DLC, Al) better because of small collisional effects, especially for thick tip case such as extended double cone or tongari cone.**
  - **Guiding field at the cone side wall is observed → possibility of extended resistive guiding cone (Toganri Cone)**
- **Tip Deformation**
  - **Strong resistive field generated at the tip head - plasma contact surface, which scatters fast electrons and reduces the heating rate. → from this point of view, low-Z material is better.**

Resistive field

At cone side wall : collimation and focusing.

At tip head : scattering (especially in deformed case)

→ **So, tip head should be located close to core, such as extended double cone or extended resistive guiding cone .**

But, How about plasma Jet effetcs??

→ **Performance evaluation for advanced cone by Integrated simulation**